

Chapter 13 – Accident Analyses ATOMIC ALCHEMY INC.

Non-Proprietary

Document Number	Revision	Approved By	Template
AAI-PSAR-13 (NP)	0		TEM-003 Rev 2 (05/14/2025)



TABLE OF CONTENTS

Terms		13-7
Acronym	and Abbreviations	13-7
13 Acci	dent Analyses	13-8
13.0 I	ntroduction	13-8
13.1	Reactor Accidents	13-8
13.1.1	Acceptance Criteria	13-8
13.1.2	Dependence on Operator Actions	13-8
13.2 I	Reactor Characteristics Considered in the Safety Evaluation	13-9
13.2.1	Meteorological Conditions Assumed in Accident Analyses	13-9
13.2.2	Facility Parameters and Initial Conditions Assumed in Accident Analyses	13-9
13.2.3	Instrumentation Drift and Calorimetric Errors, Power Range Neutron Flux	13-10
13.2.4	Identification of Conservatisms	13-10
13.2.5	Power Distribution	13-11
13.2.6	Distribution of Decay Heat	13-13
13.2.7	Fission Product Inventories	13-14
13.2.8	Control Rod Insertion Characteristics	13-14
13.2.9	Methodology	13-14
13.3 I	Description, Evaluation, and Consequences of Individual Events	13-16
13.3.1	Maximum Hypothetical Accident	13-16
13.3	.1.1 Initial Conditions	13-17
13.3	.1.2 Identification of Causes	13-17
13.3	.1.3 Sequence of Events and Systems Operation	13-17
13	3.1.3.1 Damage to Equipment	13-17
13	3.1.3.2 Core and System Performance	13-18
13	3.1.3.3 Barrier Performance	13-18
13	3.1.3.4 Radiological Consequences	13-18
13.3.2	Insertion of Excess Reactivity	13-26
13.3	·	
Read	·	
13.3	.2.2 Rapid Removal of the Most Reactive Control Rods	13-26







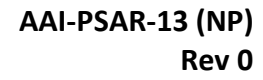
CHAPTER 13
ACCIDENT ANALYSES

13.3.2.3 Position	Rapid Insertion of a Fuel Element into a Vacancy in the Core at the Mo 13-26	st Reactive
13.3.2.3	3.1 Initial Conditions	13-26
13.3.2.3	3.2 Identification of Causes	13-27
13.3.2.3	3.3 Sequence of Events and Systems Operation	13-27
13.3.2.3	3.4 Damage to Equipment	13-27
13.3.2.3	3.5 Core and System Performance	13-28
13.3.2.3	3.6 Barrier Performance	13-30
13.3.2.3	3.7 Radiological Consequences	13-30
13.3.2.4	Ramp Insertion of Reactivity by Drive Motion of the Most Reactive Cor	
13.3.2.4	4.1 Initial Conditions	
13.3.2.4		
13.3.2.4	1.3 Sequence of Events and Systems Operation	13-31
13.3.2.4	1.4 Damage to Equipment	13-31
13.3.2.4	1.5 Core and System Performance	13-32
13.3.2.4	1.6 Barrier Performance	13-34
13.3.2.4	1.7 Radiological Consequences	13-34
13.3.2.5	Failure of an Experiment that Inserts Excess Reactivity	13-34
13.3.2.6	Rapid Increase in Reactivity as a Result of a Change in Operating Paran	neters 13-34
13.3.3 Los	ss of Coolant	13-34
13.3.3.1	Failure of a Component in the Primary Coolant Loop	13-34
13.3.3.2	Failure in the Chemical and Volume Control System	13-34
13.3.3.3	Failure of an Experimental Facility	13-35
13.3.3.4	Failure of the Primary Coolant Boundary	13-35
13.3.3.4	1.1 Initial Conditions	13-35
13.3.3.4	1.2 Identification of Causes	13-35
13.3.3.4	1.3 Sequence of Events and Systems Operation	13-35
13.3.3.4	1.4 Damage to Equipment	13-36
13.3.3.4	1.5 Core and System Performance	13-36
13.3.3.4	1.6 Barrier Performance	13-40
13.3.3.4	1.7 Radiological Consequences	13-40





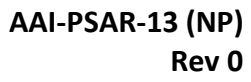
13.3.4	Loss	s of Coolant Flow	L3-41
13.3.	4.1	Loss of Electrical Power	L3-41
13.3.	4.2	Failure of a Component in the Primary Coolant System	L3-41
13.	3.4.2.	.1 Initial Conditions	L3-41
13.	3.4.2.	.2 Identification of Causes	L3-42
13.	3.4.2.	.3 Sequence of Events and Systems Operation1	L3-42
13.	3.4.2.	.4 Damage to Equipment	L3-42
13.	3.4.2.	.5 Core and System Performance1	L3-42
13.	3.4.2.	.6 Barrier Performance	L3-46
13.	3.4.2.	.7 Radiological Consequences1	L3-46
13.3.	4.3	Blocking of One or More Fuel Coolant Channels	L3-47
13.3.5	Misl	handling or Malfunction of Fuel1	L3-47
13.3.	5.1	Overheating of Fuel During Steady-Power Operation	L3-47
13.3.	5.2	Dropping or Damaging Fuel	L3-47
13.3.	5.3	Dropping of or Impacting with a Non-Fueled Component	L3-47
13.3.	5.4	Operation with Damaged Fuel	L3-47
13.3.6	Ехре	eriment Malfunction	L3-47
13.3.	6.1	Loss of Cooling Capability in a Fueled Experiment	L3-47
13.3.	6.2	Mechanical Failure of a Fueled Experiment – Maximum Credible Accident	L3-47
13.	3.6.2.	1 Initial Conditions and Methodology	L3-47
13.	3.6.2.	.2 Accident Initiator and Scenario Evolution	L3-48
13.	3.6.2.	.3 Sequence of Events and Timing1	L3-48
13.	3.6.2.	.4 Barrier Failures and Releases	L3-48
13.	3.6.2.	.5 Source Term Derivation1	L3-49
13.	3.6.2.	.6 Occupational Dose Calculation1	L3-49
13.	3.6.2.	.7 Offsite Dose Calculation	L3-49
13.	3.6.2.	.8 Occupational and Offsite Dose Results1	L3-50
13.	3.6.2.	.9 Comparison to Dose Acceptance Criteria	13-50
13.3.	6.3	Loss of Cooling Capability in a Strongly Absorbing Non-Fueled Experiment	13-51
13.3.	6.4	Placement of an Experiment Component in an Unplanned Location	13-51
13.3.	6.5	Failure of an Experiment Containing Highly Reactive Contents	13-51





Page 13-5

13.3	.6.6	Failure of an Experiment and Release of Corrosive Materials into the Reactor Co	
13.3	.6.7	Detonation of an Explosive Experiment	13-51
13.3.7	Loss	s of Normal Electrical Power	13-51
13.3.8	Exte	ernal Events	13-51
13.3	.8.1	Meteorological Disturbance	13-51
13.3	.8.2	Seismic Event	13-52
13.3	.8.3	Mechanical Impact or Collision with Building	13-52
13.3.9	Mis	handling or Malfunction of Equipment	
13.3	.9.1	Operator Error at the Controls	13-52
13.3	.9.2	Other Operator Errors	
13.3	.9.3	Malfunction or Loss of Safety-Related Instruments or Controls	13-52
13.3	.9.4	Electrical Fault in Control Rod Systems	
13.3	.9.5	Malfunction of Confinement or Containment System	
13.3	.9.6	Rapid Leak of Contaminated Liquid	
13.4	Summ	nary and Conclusions	
13.5 F	Refere	ences	13-53
		LIST OF FIGURES	
Figure 13-1:	Noda	al diagram of the RELAP5 model	13-16
_	-	reactivity insertion accident hot pin fuel centerline temperature response	
_	•	reactivity insertion accident hot pin cladding temperature response	
_	•	reactivity insertion accident bulk coolant core exit temperature response	
_		p reactivity insertion accident hot pin fuel centerline temperature response	
		p reactivity insertion accident hot pin cladding temperature response	
•		of coolant accident hot pin fuel centerline temperature response	
_		of coolant accident hot pin cladding temperature response	
_		s of coolant accident bulk coolant core exit temperature response	
•		s of coolant accident bulk coolant core inlet velocity response	
_		pin and bulk coolant temperatures following a loss of coolant accident	
Figure 13-13	3: Los	s of coolant flow accident hot pin fuel centerline temperature response	13-43
Figure 13-14	4: Los	s of coolant flow accident hot pin cladding temperature response	13-44
_		s of coolant flow accident bulk coolant core exit temperature response	
_		s of coolant flow accident bulk coolant velocity and void fraction response in the	
		pin bulk coolant temperatures following a loss of coolant flow accident	
ココピロロモ エンニー	,	- MILLOUIS COMBILLEUDELBUIES IUNOWINE BIUSS UL CUUBIII HUW BULUEIII	. , , - 4 ()







ACCIDENT ANALYSES

CHAPTER 13

LIST OF TABLES

Table 13-1: Reactor module characteristics considered in the safety evaluation	13-9
Table 13-2: Reactor protection system setpoints	13-10
Table 13-3: Reactor scram signal time delays assumed in the VIPR accident analyses	13-10
Table 13-4: Parameters used in the iterative calculation of the reactor's power, temperature	e, and
density distributions	
Table 13-5: MHA source term	
Table 13-6: DDE and CEDE factors used in the MHA analysis	
Table 13-7: Parameters used in the offsite dose consequence assessment	
Table 13-8: Activity exhaust rates	
Table 13-9: Results of the offsite 24-hour dose consequence assessment at 150 m	13-26
Table 13-10: Step reactivity insertion accident output parameters	
Table 13-11: Ramp reactivity insertion accident output parameters	13-34
Table 13-12: Loss of coolant accident output parameters	
Table 13-13: Loss of coolant flow accident output parameters	
Table 13-14: Factors from RG 1.183 Rev. 1 (2023) Table 4 and actinides	
Table 13-15: Occupational and offsite TEDE and thyroid dose results from the MCA	13-50
Table 13-16: Comparison of dose results to acceptance criteria and outcomes	13-50
LIST OF EQUATIONS	
·	. 42.42
Equation 13-1: Axial coolant temperatures as a function of fuel pin linear heat generation ra	
Equation 13-2: Axial fuel temperatures as a function of fuel pin linear heat generation rate	
Equation 13-3: UO ₂ thermal conductivity fit	
Equation 13-4: Shutdown decay power equations	
Equation 13-5: Combined dose consequences	13-23



AAI-PSAR-13 (NP) Rev 0

Page 13-7

TERMS

ACRONYMS AND ABBREVIATIONS

Common acronyms, abbreviations, and units of measurements may not be included here as it is assumed the reader is familiar with their meaning.

AAI Atomic Alchemy Inc.

CEDE committed effective dose equivalent

CFR Code of Federal Regulation

DDE deep dose equivalent

DNBR departure from nucleate boiling ratio

EPZ emergency planning zone

FGR Federal Guidance Report

IAEA International Atomic Energy Agency

INL Idaho National Laboratory

MCA Maximum Credible Accident

MHA Maximum Hypothetical Accident

NOAA U.S. National Oceanic and Atmospheric Administration

NPUF Non-Power Production or Utilization Facility

PCS primary coolant system

PWR pressurized water reactor

RG Regulatory Guide

TEDE total effective dose equivalent

VIPR Versatile Isotope Production Reactor

χ/Q atmospheric dispersion value



AAI-PSAR-13 (NP) Rev 0

Page 13-8

13 ACCIDENT ANALYSES

13.0 INTRODUCTION

This chapter presents analyses that show that the health and safety of the public and workers are protected and that Atomic Alchemy Inc. (AAI) has considered potential radiological consequences in the event of malfunctions and the capability of the facility to accommodate such disturbances. The major purpose of this chapter is for AAI to demonstrate that the facility design features, safety limits, limiting safety system settings, and limiting conditions for operation have been selected to ensure that no credible accident could lead to unacceptable radiological consequences to people or the human environment.

Herein, AAI shows that operation of the facility does not pose an undue risk to the health and safety of the public, and that an incredible Maximum Hypothetical Accident (MHA) does not result in an offsite radiological dose that exceeds the 1 rem criterion set forth in Title 10 of the *Code of Federal Regulations* (CFR) 50.34(a)(1)(i), "Contents of applications; technical information" and bounds all credible accident scenarios.

13.1 REACTOR ACCIDENTS

Atomic Alchemy considers events in the following categories in the analyses presented in section 13.3:

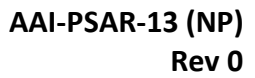
- 1. Maximum hypothetical accident
- 2. Insertion of excess reactivity
- 3. Loss of coolant
- 4. Loss of coolant flow
- 5. Mishandling or malfunction of fuel
- 6. Experiment malfunction
- 7. Loss of normal electrical power
- 8. External events
- 9. Mishandling or malfunction of equipment

13.1.1 Acceptance Criteria

Temperatures will remain below failure limits in all postulated accidents to ensure that fuel and cladding integrity is maintained and dose limits will remain below the 1 rem criterion set forth in 10 CFR 50.34.

13.1.2 <u>Dependence on Operator Actions</u>

No operator actions are necessary for a minimum of 72 hours following a design basis event. No operator actions are required to ensure reactivity control, core heat removal, or reactor confinement, reactor auxiliary, or radioisotope production facility isolation and integrity. Return to normal operation requires deliberate operator actions. The reactor trip breakers cannot be reset while a reactor trip signal is present in the safety system.







13.2 REACTOR CHARACTERISTICS CONSIDERED IN THE SAFETY EVALUATION

13.2.1 Meteorological Conditions Assumed in Accident Analyses

Meteorological conditions used in accident analyses are supported with hourly data taken by the U.S. National Oceanic and Atmospheric Administration's Idaho National Laboratory (NOAA INL) Mesonet at the Materials and Fuels Complex sampling station. Over 2 years of hourly data were retrieved for use in plume calculations in the analysis of the MHA in Section 13.3.1. This data covers the time period from 2020-06-22 15:00:00 to 2022-12-22 15:00:00. Data from the NOAA INL Mesonet satisfies the guidance given in NRC Regulatory Guide (RG) 1.23, "Meteorological Monitoring Programs for Nuclear Power Plants," and is suitable for use in these accident analyses.

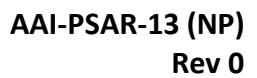
The data used for the meteorological conditions assumed in the accident analysis can be found in Chapter 2, Section 2.3.2.

13.2.2 <u>Facility Parameters and Initial Conditions Assumed in Accident Analyses</u>

Data used in the subsequent accident analyses, particularly core neutronic and thermal hydraulic data, are given in **Table** 13-1. **Table** 13-2 and **Table** 13-3 give relevant protection & monitoring system setpoints and scram signal delays, respectively.

Table 13-1: Reactor module characteristics considered in the safety evaluation

Parameter	Value	Unit
Power	16.80	MW
Moderator Temperature Coefficient of Reactivity	-6.09	pcm °C ⁻¹
Moderator Void Coefficient of Reactivity	-153.61	pcm Δ% _{void} -1
Fuel Temperature Coefficient of Reactivity	-1.35	pcm °C ⁻¹
Effective Neutron Lifetime	5.13×10 ⁻⁵	S
Delayed Neutron Lifetime	4.96×10 ⁻¹	S
Steady State Heat Flux (Average)	60.10	W cm ⁻²
Steady State Heat Flux (Maximum)	153.78	W cm ⁻²
Steady State DNBR	3.71	
Core Coolant Flow Rate	[]PROP	kg s ⁻¹
Core Coolant Inlet Temperature	[]PROP	°C
Core Coolant Average Exit Temperature	55	°C
Steady State Fuel Centerline Temperature	2358	°C





Page 13-10

Parameter	Value	Unit
Reactor Coolant System Inventory	322	m³
Control Rod Worth, Differential	232	pcm cm ⁻¹
Control Rod Worth, Total	12853	pcm

Table 13-2: Reactor protection system setpoints

Setpoint	Nominal Value	Setpoint Value	Unit
Reactor Overpower	15.00	16.80	MW
Low Primary Coolant Flow	[]PROP	[]PROP	kg/s
Pool Surface Area Radiation Monitor	To be address	in the FSAR	mrem/h
Reactor Inlet Temperature	[]PROP	[]PROP	°C

Table 13-3: Reactor scram signal time delays assumed in the VIPR accident analyses

Delay	Value	Unit
Reactor Scram Signal	1.00	S

13.2.3 Instrumentation Drift and Calorimetric Errors, Power Range Neutron Flux

This section will be further developed in the FSAR as these values are dependent on final design and equipment chosen.

13.2.4 Identification of Conservatisms

Accident analyses were conducted using the most conservative initial conditions, including, when applicable:

- Fresh, undepleted fuel in all Versatile Isotope Production Reactor (VIPR) fuel assembly positions
 - In this configuration, which would occur only at the start of the first VIPR fuel cycle, the greatest quantity of fissile fuel and absence of fission product poisons result in the highest available excess reactivity. This state results in higher power densities, higher maximum temperatures, the minimum shutdown margin provided by the reactivity control system, and larger and more rapid potential power excursions.



AAI-PSAR-13 (NP) Rev 0

Page 13-11

No fissile isotope-containing irradiation targets present

The presence of fissile isotope-containing irradiation targets used in the production of some radioisotopes, shifts a fraction of the total thermal power production away from the VIPR fuel. Conducting accident analyses without heat-producing targets present increases power densities in the VIPR core.

Hot full power

The system begins the accident closer to its design limits than otherwise, and more latent thermal energy is present that must be dissipated following the accident. Modeling of the reactor at its maximum licensed power level, rather than the intended operational power, provides additional conservatism.

Fission product inventories determined at 16.8 MW operating power and a burnup of
 []PROP,ECI

The VIPR, while licensed for a maximum thermal operating power of 16.8 MW, is intended to be operated at 15 MW. The average burnup predicted for a fuel assembly in the VIPR core is [] PROP,ECI . Fission product inventories calculated at 16.8 MW and [] PROP,ECI are higher than those expected at any time in the VIPR.

Timing delays in reactor scram circuit

Estimates of the delay in a reactor scram from any source are on the order of tenths of one second. Accident analyses assume a one second delay between the violation of any safety monitoring setpoint and the initiation of the reactor scram.

Further details on related uncertainties, margins of safety, as well as validation of the computational models and codes, which are discussed herein and in Chapter 4 (i.e., Serpent 2 and RELAP5), will be provided in the FSAR, as appropriate.

13.2.5 Power Distribution

Table 13-4 below defines the parameters used in the iterative coupling of thermal-hydraulic and neutronic calculations to establish steady-state temperature and coolant density distributions. These parameters were used to evaluate fuel and coolant temperatures as functions of local linear heat generation rates, which in turn depend on the power distribution calculated by Serpent 2. Temperature-dependent properties such as fuel thermal conductivity and coolant density were updated in each iteration and fed back into the neutronic model until convergence was achieved across all distributions. This iterative approach ensures a self-consistent solution that accurately reflects the coupled behavior of the reactor core under steady-state conditions.

The radial and axial thermal power distributions described in Chapter 4 were used in all hot full power VIPR accident analyses. These distributions were obtained through stochastic simulation of the VIPR core in the Serpent 2 code. In those analyses where the initial condition of the VIPR is not hot full power, similar distributions were calculated for the appropriate power levels.



The predicted power distributions were used in external fuel temperature, coolant temperature, and coolant density calculations to determine the corresponding initial temperature and density distributions. The following equations and parameters were used:

$$T_m(z) = T_0 + \sum_{n=0}^{z} \frac{q'_n}{\dot{m}c_p}$$

Equation 13-1: Axial coolant temperatures as a function of fuel pin linear heat generation rate

$$T_f(z) = \frac{q'(z)}{2\pi} \left[\frac{1}{2k_f(T_f)} + \frac{1}{R_a h_a} + \frac{1}{k_c} ln\left(\frac{R_{co}}{R_{ci}}\right) + \frac{1}{R_{oo} k_o/\delta_o} + \frac{1}{R_{oo} h} \right] + T_m(z)$$

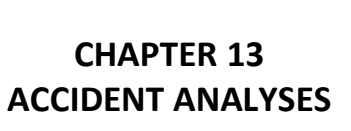
Equation 13-2: Axial fuel temperatures as a function of fuel pin linear heat generation rate

$$k_f = \begin{bmatrix} 1.31219 \times 10^{-1} \\ -2.23378 \times 10^{-4} T_f(z) \\ +2.03101 \times 10^{-7} T_f(z)^2 \\ -9.90270 \times 10^{-11} T_f(z)^3 \\ +2.47295 \times 10^{-14} T_f(z)^4 \\ -2.42534 \times 10^{-18} T_f(z)^5 \end{bmatrix}$$

Equation 13-3: UO₂ thermal conductivity fit

Table 13-4: Parameters used in the iterative calculation of the reactor's power, temperature, and density distributions

Symbol	Parameter	Unit
T_m	Coolant Temperature	°C
T_f	Fuel Centerline Temperature	°C
T_0	Coolant Inlet Temperature	°C
ρ_m	Coolant Density	g/cm ³
q'	Linear Heat Generation	W/cm
ṁ	Coolant Mass Flow Rate	kg/s
c_p	Coolant Specific Heat Capacity	J/(g °C)
k_f	Fuel Thermal Conductivity	W/(cm °C)
R_g	Gap Mid-Radius	cm





Symbol	Parameter	Unit
h_g	Gap Conductance	W/(cm ² °C)
k_c	Cladding Thermal Conductivity	W/(cm °C)
R_{co}	Cladding Outer Radius	cm
R_{ci}	Cladding Inner Radius	cm
Roo	Oxide Radius	cm
k_o	Oxide Thermal Conductivity	W/(cm °C)
δ_o	Oxide Thickness	cm
h	Cladding-Coolant Heat Transfer Coefficient	W/(cm ² °C)

Coolant density as a function of temperature was predicted by interpolating between data obtained from The National Institute of Standards and Technology for the isobaric properties of light water at 202.65 kPa.

The temperature and density distributions were returned to the Serpent simulation and used to calculate updated power distributions. Simulations and calculations were iterated until convergence was reached in all distributions.

Accident analyses involving thermal hydraulic simulations in RELAP5 further modified the utilized power distributions. Radial distributions were divided into two groups: those powers which belonged to the hot pin in the VIPR core, and those that did not. This division produced two axial power distributions which were utilized in the thermal hydraulic models: an axial hot pin power distribution, and an axial bulk fuel power distribution. This allowed the analyses to identify both the most limiting and the average behavior over the duration of each modeled accident.

13.2.6 Distribution of Decay Heat

Decay heat modeling enables accurate predictions of core thermal behavior following reactor shutdown especially where active cooling is degraded or lost. This section describes the methods used to characterize decay power evolution for thermal-hydraulic and safety analyses.

In accident analyses where the decay heat produced by the system was relevant, either of two models was utilized. In RELAP5 analyses involving a time-dependent change in the reactivity of the system, the default decay heat model provided by the code was used. Otherwise, a decay heat factor was calculated according to the following set of equations:

$$\frac{P(t_s)}{P_0} = -6.14575 \times 10^{-3} \ln(t_s) + 0.060157 \text{ for } 1.5 \le t_s \le 400 \text{ s}$$

$$\frac{P(t_s)}{P_0} = 1.40680 \times 10^{-1} t_s^{-0.286} \text{ for } 400 < t_s \le 4 \times 10^5 \text{ s}$$





CHAPTER 13 **ACCIDENT ANALYSES**

$$\begin{split} \frac{P(t_s)}{P_0} &= 8.70300 \times 10^{-1} t_s^{-0.4255} \text{ for } 4 \times 10^5 < t_s \le 4 \times 10^6 \text{ s} \\ \frac{P(t_s)}{P_0} &= 1.28420 \times 10^1 t_s^{-0.6014} \text{ for } 4 \times 10^6 < t_s \le 4 \times 10^7 \text{ s} \\ \frac{P(t_s)}{P_0} &= 4.03830 \times 10^4 t_s^{-1.0675} \text{ for } 4 \times 10^7 < t_s \le 4 \times 10^8 \text{ s} \\ \frac{P(t_s)}{P_0} &= 3.91130 \times 10^{-5} \exp(7.3541 \times 10^{-10} t_s) \text{ for } 4 \times 10^8 < t_s \le 10^{10} \text{ s}, \end{split}$$

Equation 13-4: Shutdown decay power equations

In these equations, t_s is the time since reactor shutdown, in seconds. These equations, determined by Todreas and Kazimi, are a fit to the tabular decay heat power data given in ANSI/ANS-5.1-2005, "Decay Heat Power in Light Water Reactors."

13.2.7 **Fission Product Inventories**

Accidents involving the radioactive dose contribution of fission products utilized fission product inventories determined from the stochastic simulation of the VIPR core in the Serpent 2 code, with the PROP,ECI reactor modeled at 16.8 MWth operating power and a burnup of [

In accidents where the integrity of the fuel and cladding was not violated, the simulation of fresh, undepleted fuel containing no fission products was determined to be more conservative and was used in the analyses.

13.2.8 **Control Rod Insertion Characteristics**

Stochastic simulations of the neutron multiplication of the VIPR core with the control rods at incremental heights were run in the Serpent 2 code. A polynomial fit was made to the data to produce an integral control rod worth curve. Worth curves were determined for the individual control rod and reg rod groups, all of the control rod groups together, and all of the control rod groups without the highest worth group.

The maximum rate of reactivity insertion allowed is 69 pcm/s (0.10 \$/s), corresponding to the simultaneous movement of all control rod assemblies at 0.17 cm/s.

The control rods assemblies are designed to, under the conditions of a reactor scram, fall into the reactor under the force of gravity. All analyses involving control rod drop kinetics assume the control rod assemblies fall under gravitational acceleration and with a conservative scram delay of 1.0 second.

13.2.9 Methodology

RELAP5 Mod 3.3 was selected as the primary simulation tool based on its established applicability for modeling two-phase flow and transient heat transfer in reactor systems. RELAP5 models are used to calculate temperatures, heat fluxes, and boiling conditions in the reactor core, particularly in bounding hot channel scenarios (e.g. hot pin). To support these simulations, neutronic and radiological input



AAI-PSAR-13 (NP) Rev 0

Page 13-15

data (including decay heat profiles, control rod worths, and time-resolved radionuclide inventories) were developed using the Serpent 2 Monte Carlo code.

Although no dynamic coupling is performed during time-dependent simulations, steady-state core conditions and radiological source terms are precomputed in Serpent and used as fixed inputs to RELAP5 analyses. RELAP5 is used to model the fluid and thermal behavior of the VIPR core and primary coolant system (PCS) during normal operation and accident conditions. This offline integration ensures that core power distributions and fission product inventories used in accident scenarios reflect a physically consistent reactor state at the time of the event.

The RELAP5 model evaluates the performance of the entire coolant loop and the hot fuel pin in the reactor to ensure the general performance and safety of the reactor. The model initial conditions are set to the parameters established in **Table 13-1**. The PCS nodal diagram that was used in the thermal hydraulic analysis for the cooling of the core is depicted in **Figure 13-1** and is representative of the developed RELAP5 model. The time-dependent volume above the pool represents the atmospheric pressure and temperature that is held in the building. The secondary loop consists of a time-dependent volume and time-dependent junction to a pipe connected through a heat structure representing the heat exchanger to the PCS. The fuel is separated into two separate heat structures to monitor the behavior of the hot fuel pin and the average performance in the reactor core. For the accident scenarios modeled, the bounding performance of the hot fuel pin is assessed to ensure the reactor meets the acceptance criteria.



AAI-PSAR-13 (NP) Rev 0

Page 13-16

[PROP,ECI

Figure 13-1: Nodal diagram of the RELAP5 model

The reactor design has a passive cooling feature that allows a natural convection loop to cool the core during normal and abnormal shutdown conditions. The passive inlet ports are not considered safety-related and are not relied upon for any accident scenarios.

13.3 DESCRIPTION, EVALUATION, AND CONSEQUENCES OF INDIVIDUAL EVENTS

13.3.1 <u>Maximum Hypothetical Accident</u>

The analysis of the MHA establishes a bounding event where, even in an incredible scenario resulting in the release of fission products to the atmosphere, safe reactor shutdown and protection of the public, the operations and user staff, and the environment are ensured. The MHA for the AAI facility is



AAI-PSAR-13 (NP) Rev 0

Page 13-17

the cladding failure of every fuel pin in a single VIPR fuel assembly, assumed to be caused by a fuel handling accident in the reactor pool. The hypothesized fuel handling accident shears through each of the fuel pins in the affected assembly, compromising the cladding integrity and releasing the entire inventory of gaseous fission products from each pin. More realistically a fuel handling accident, defined as dropping and damaging a used fuel assembly, would involve a small number of damaged fuel pins, if any. The analysis is informed by the methodology outlined in RG 1.183.

Because the VIPR uses []PROP,ECI fuel assemblies, regulatory guidance relating to fuel handling accidents in PWRs is used for this analysis, where applicable.

13.3.1.1 Initial Conditions

For this accident analysis, the fission product inventory of the affected fuel assembly was determined by simulation of the VIPR in Serpent at 16 MW for [] PROP, to allow dosesignificant radionuclides to reach equilibrium or bounding maximum values. The accident was assumed to occur immediately after reactor shutdown, with no radioactive decay of fission products credited before the onset the MHA. The depth of the reactor pool was assumed to be at its limiting safety system setting of [] PROP.

13.3.1.2 Identification of Causes

A potential cause of the fuel handling error is an unspecified failure of the fuel handling machine or human error, causing the affected fuel assembly to drop. However, because it is unlikely for this accident to result in consequences of the magnitude considered in this analysis, it was assumed that the fuel assembly is spontaneously sheared through with no specific cause.

13.3.1.3 Sequence of Events and Systems Operation

The anticipated sequence of events which would occur for a bounding, postulated []PROP,ECI pin failure are as follows:

The accident was assumed to occur immediately after reactor shutdown.

Gaseous fission products were assumed to be transported instantly from the damaged fuel, through the reactor pool, and into the reactor building atmosphere. For the purposes of the PSAR, the activities were assumed to immediately disperse homogeneously throughout the air volume of the confinement to produce air concentrations to be treated as a ground-level release at the assumed leakage rate. The contaminated gases were assumed to immediately begin leaking from the building.

The fission product release scenario was assumed to last 24 hours, with a receptor located offsite exposed to the plume of radioactive material during this time. The total dose accumulated by the receptor over this time was calculated.

13.3.1.3.1 Damage to Equipment

Aside from the damaged fuel assembly, no damage to other equipment was assumed in this scenario. Due to its design, slow transfer movement, and low lift height, it is not postulated that the fuel assembly would be capable of puncturing the stainless steel pool liner. Used fuel is stored in a pattern that precludes assemblies being moved above other assemblies in the used fuel storage pool.



AAI-PSAR-13 (NP) Rev 0

Page 13-18

13.3.1.3.2 Core and System Performance

The accident takes place outside of the reactor core and would occur when the reactor is not operating.

13.3.1.3.3 Barrier Performance

Radionuclide-containing gases in this scenario leak from the reactor building at ground level and at a leak rate proportional to the internal volume of the building. No credit is taken for filtration of the escaping gases.

13.3.1.3.4 Radiological Consequences

This section presents the evaluation of offsite dose consequences resulting from the MHA. Radiological consequences are evaluated in terms of total effective dose equivalent (TEDE) to offsite receptors, consistent with the requirements of 10 CFR 50.34(a)(1)(i).

Atmospheric dispersion modeling supporting this analysis is based on site-specific, hourly meteorological data and uses 0.5% exceedance atmospheric dispersion value (χ /Q) bounding stability class assumptions. For the MHA, a 24-hour integration period is assumed to conservatively represent unfiltered confinement leakage.

The MHA source term was determined as informed by the guidance given in Regulatory Position 3 of RG 1.183 related to fuel handling accidents and Appendix B to RG 1.183. The total core inventory was determined with the isotope generation and depletion features of Serpent 2. The total core inventory was divided by []^{PROP} to reflect the inventory of a single fuel assembly, multiplied by an assembly peaking factor of 1.034 to reflect the greater inventory of the highest power fuel assembly, and multiplied by an uncertainty factor of 1.02 in accordance with Appendix K to 10 CFR Part 50, "Domestic Licensing of Production and Utilization Facilities."

To account for radioactive decay and the potential ingrowth of radionuclides to greater than equilibrium levels after reactor shutdown, Serpent was used to decay the initial inventory at successive timesteps throughout the accident. Although only radionuclides belonging to the groups specified in Table 4 of Regulatory Guide (RG) 1.183, "Alternative Radiological Source Terms For Evaluating Design Basis Accidents at Nuclear Power Reactors," issued July 2000, were considered, all nuclides for which data was available to Serpent were tracked to account for all possible sources of ingrowth for the considered radionuclides. The length of each timestep was increased occasionally at times later in the accident progression.

The affected fuel assembly inventory, with the discussed correction factors applied, is tabulated in **Table** 13-5. The list of radionuclides is reduced to only those that contribute to the cumulative dose at the receptor at any point during the accident (e.g. only radionuclides with a nonzero effective or deep dose equivalent (DDE) or committed effective dose equivalent (CEDE) and with nonzero activity at any



CHAPTER 13
ACCIDENT ANALYSES

timestep). Only halogens and noble gases were considered in the MHA release, as all other fission products were assumed to be retained in the fuel or in particulate form and retained by the water in the reactor pool. All halogen and noble gas isotopes tracked by Serpent with DDE or CEDE factors provided in Table III.1 of Federal Guidance Report 12 and Table 2.1 of Federal Guidance Report 11, respectively, were considered. Among the CEDE dose conversion factors, different lung clearance classes are given for common radionuclide chemical forms; the most conservative values were chosen. The DDE and CEDE factors used in the MHA analysis are given in **Table** 13-6. As with the radionuclide inventory, the list of factors is reduced to only those radionuclides that contribute to the cumulative dose at the receptor at any point during the accident.

Table 13-5: MHA source term

Nuclide	Start (0 s)	24 Hours (86400 s)
Nuclide	Assembly Activity (Bq)	Assembly Activity (Bq)
Br-75	1.22E-01	4.00E-06
Br-76	1.38E-10	4.94E-11
Br-77	8.26E+03	6.17E+03
Br-80	2.52E+09	1.70E+07
Br-80m	6.82E+08	1.58E+07
Br-82	5.23E+12	3.27E+12
Br-83	2.08E+14	2.37E+11
Br-84	3.51E+14	8.76E+00
Kr-77	1.54E-03	2.29E-09
Kr-79	6.47E+03	4.02E+03
Kr-81	7.03E+02	7.03E+02
Kr-81m	4.20E+07	4.21E+01
Kr-83m	2.09E+14	9.04E+11
Kr-85	3.40E+13	3.40E+13
Kr-85m	4.74E+14	1.17E+13
Kr-87	8.67E+14	1.82E+09
Kr-88	1.14E+15	3.26E+12
I-121	1.13E+01	4.43E-03
I-122	2.94E-11	0.00E+00
I-123	3.35E+04	9.53E+03





CHAPTER 13 ACCIDENT ANALYSES

Nuclide	Start (0 s)	24 Hours (86400 s)
Nucliue	Assembly Activity (Bq)	Assembly Activity (Bq)
I-124	2.90E-02	2.46E-02
I-125	2.51E+06	2.48E+06
I-126	1.62E+09	1.53E+09
I-128	1.65E+13	7.42E-05
I-129	7.44E+07	7.44E+07
I-130	4.56E+13	1.19E+13
I-131	1.81E+15	1.69E+15
I-132	2.61E+15	2.11E+15
I-132m	3.62E+13	2.24E+08
I-133	3.66E+15	1.69E+15
I-134	4.08E+15	9.07E+07
I-135	3.47E+15	2.76E+14
Xe-122	2.94E-11	1.29E-11
Xe-123	5.77E-07	1.94E-10
Xe-125	2.04E+03	7.61E+02
Xe-127	5.90E+07	5.79E+07
Xe-129m	1.64E+10	1.52E+10
Xe-131m	1.99E+13	1.98E+13
Xe-133	3.69E+15	3.55E+15
Xe-133m	1.15E+14	1.03E+14
Xe-135	8.05E+14	8.69E+14
Xe-135m	8.00E+14	4.75E+13
Xe-138	3.07E+15	0.00E+00
Total	2.75E+16	1.04E+16



Table 13-6: DDE and CEDE factors used in the MHA analysis

Nuclide	CEDE factors used in the MHA analysis Effective		
Nucliue	DDE (rem m³/Bq s)	CEDE (rem/Bq)	
Br-75	5.84E-12	3.54E-09	
Br-76	1.34E-11	4.32E-08	
Br-77	1.51E-12	7.46E-09	
Br-80	3.85E-13	7.62E-10	
Br-80m	3.11E-14	1.06E-08	
Br-82	1.30E-11	4.13E-08	
Br-83	3.82E-14	2.41E-09	
Br-84	9.41E-12	2.61E-09	
Kr-77	4.86E-12	0.00E+00	
Kr-79	1.21E-12	0.00E+00	
Kr-81	2.67E-14	0.00E+00	
Kr-81m	6.14E-13	0.00E+00	
Kr-83m	1.50E-16	0.00E+00	
Kr-85	1.19E-14	0.00E+00	
Kr-85m	7.48E-13	0.00E+00	
Kr-87	4.12E-12	0.00E+00	
Kr-88	1.02E-11	0.00E+00	
I-121	1.94E-12	3.21E-09	
I-122	4.56E-12	0.00E+00	
I-123	7.28E-13	8.01E-09	
I-124	5.38E-12	5.23E-07	
I-125	5.22E-14	6.53E-07	
I-126	2.15E-12	1.20E-06	
I-128	4.16E-13	1.28E-09	
I-129	3.80E-14	4.69E-06	
I-130	1.04E-11	7.14E-08	
I-131	1.82E-12	8.89E-07	





Nuclide	Effective		
Nucliue	DDE (rem m³/Bq s)	CEDE (rem/Bq)	
I-132	1.12E-11	1.03E-08	
I-132m	1.53E-12	8.10E-09	
I-133	2.94E-12	1.58E-07	
I-134	1.30E-11	3.55E-09	
I-135	7.98E-12	3.32E-08	
Xe-122	2.46E-13	0.00E+00	
Xe-123	3.03E-12	0.00E+00	
Xe-125	1.19E-12	0.00E+00	
Xe-127	1.25E-12	0.00E+00	
Xe-129m	1.06E-13	0.00E+00	
Xe-131m	3.89E-14	0.00E+00	
Xe-133	1.56E-13	0.00E+00	
Xe-133m	1.37E-13	0.00E+00	
Xe-135	1.19E-12	0.00E+00	
Xe-135m	2.04E-12	0.00E+00	

CHAPTER 13

ACCIDENT ANALYSES

The entirety of the gap activity in the damaged fuel assembly was assumed to be instantly released to the pool, instantly transported to the building atmosphere, uniformly dispersed, and released to the environment over the 24 h time period.

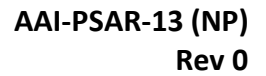
0.00E+00

5.77E-12

Xe-138

Dose consequences at the site boundary were determined through analysis of the plume transport and dispersion by calculation of an effective χ/Q . χ/Q values used in the MHA analysis was calculated by following the methodologies provided in RG 1.145, "Atmospheric Dispersion Models for Potential Accident Consequence Assessments at Nuclear Power Plants" Rev 1, issued November 1983, reviewed 2014, RG 1.111, "Methods for Estimation Atmospheric Transport and Dispersion of Gaseous Effluents in Routine Releases from Light-Water-Cooled Reactor" Rev 1, issued July 1977, and NOAA Tech Memo ERL-ARL-42.

 χ /Q values in Chapter 2 were calculated at the site boundary distance within each of 16 directional sectors for ground releases. The value exceeded 0.5 percent of the time in each sector, and the highest of these was chosen as the χ /Q value.





Dose consequences to a particular organ from internal and external exposure to a particular radionuclide were calculated according to:

$$D_{n,o,t} = A_{n,t} \times \Delta T_t \times \frac{\chi}{Q} \times \left(DDE_{n,o} + CEDE_{n,o} \times BR_t\right)$$

Equation 13-5: Combined dose consequences

In this equation, $D_{n,o,t}$ is the dose to organ o from radionuclide n at each timestep, $A_{n,t}$ is the activity exhaust rate of radionuclide n, ΔT_t is the length of timestep t, χ/Q is the atmospheric dispersion value at the given receptor distance, $DDE_{n,o}$ is the deep dose equivalent for organ o from radionuclide n, $CEDE_{n,o}$ is the committed effective dose equivalent for organ o from radionuclide n, and BR_t is the breathing rate of the exposed individual. The total effective dose at each timestep was calculated by summing the individual contributions of all radionuclides. The total dose over the course of the accident was obtained by summing the dose uptake at all timesteps.

Parameters used in the offsite dose consequence assessment are given in **Table** 13-7. Released radionuclide activity rates and results of the analysis are given in **Table** 13-8 and **Table** 13-9, respectively.

Table 13-7: Parameters used in the offsite dose consequence assessment

	Paramete	r	Value	Unit	Reference
		I-131	0.07		RG 1.183
		I-132	0.07		RG 1.183
	Gap Fraction	Kr-85	0.40		RG 1.183
	Gap i raction	Other Noble Gases	0.06		RG 1.183
		Other Halogens	0.04		RG 1.183
Source		Alkali Metals	0.20		RG 1.183
		Iodine	200		RG 1.183
	Decontamination Factor	Noble Gases	1		RG 1.183
		Particulates	Infinite		RG 1.183
	Fission Product	Irradiation Period	1300	d	
	Inventory	Thermal Power	16.00	MW	
		Leak Rate	2.40	‰ _{vol} /h	
Plume	Building	Reactor Building Width	16.76	m	
Modeling		Reactor Building Depth	76.20	m	
		Reactor Building Height Above Grade	9.14	m	





Page 13-24

Parameter		Value	Unit	Reference	
	Receptor Distance	Site Boundary	150.00	m	
	MHA Timeline	Reactor Shutdown	0	S	
Dose Consequences		Accident Initiation	0	S	
		Accident Cessation	86400	S	
	Breathing Rate	< 8 h	3.50×10 ⁻⁴	m³/s	RG 1.183
	breatining Nate	≤ 24 h	1.80×10 ⁻⁴	m³/s	RG 1.183

Table 13-8: Activity exhaust rates

Nuclide	Start (0 s)	24 Hours (86400 s)
Nucliue	Exhaust Rate (Bq/s)	Exhaust Rate (Bq/s)
Br-75	2.60E-09	5.43E-14
Br-76	2.96E-18	6.71E-19
Br-77	1.77E-04	8.38E-05
Br-80	5.39E+01	2.30E-01
Br-80m	1.46E+01	2.15E-01
Br-82	1.12E+05	4.44E+04
Br-83	4.46E+06	3.22E+03
Br-84	7.51E+06	1.19E-07
Kr-77	6.57E-09	6.21E-15
Kr-79	2.77E-02	1.09E-02
Kr-81	3.01E-03	1.91E-03
Kr-81m	1.80E+02	1.14E-04
Kr-83m	8.93E+08	2.46E+06
Kr-85	2.91E+08	1.85E+08
Kr-85m	2.03E+09	3.18E+07
Kr-87	3.71E+09	4.95E+03
Kr-88	4.89E+09	8.86E+06
I-121	2.42E-07	6.01E-11
I-122	6.30E-19	0.00E+00





Nuclide	Start (0 s)	24 Hours (86400 s)
Nucliue	Exhaust Rate (Bq/s)	Exhaust Rate (Bq/s)
I-123	7.18E-04	1.29E-04
I-124	6.20E-10	3.33E-10
I-125	5.37E-02	3.37E-02
I-126	3.46E+01	2.08E+01
I-128	3.53E+05	1.01E-12
I-129	1.59E+00	1.01E+00
I-130	9.76E+05	1.62E+05
I-131	6.21E+07	3.68E+07
I-132	5.60E+07	2.86E+07
I-132m	7.75E+05	3.04E+00
I-133	7.83E+07	2.30E+07
I-134	8.72E+07	1.23E+00
I-135	7.43E+07	3.75E+06
Xe-122	1.26E-16	3.49E-17
Xe-123	2.47E-12	5.28E-16
Xe-125	8.71E-03	2.07E-03
Xe-127	2.53E+02	1.57E+02
Xe-129m	7.04E+04	4.13E+04
Xe-131m	8.50E+07	5.38E+07
Xe-133	1.58E+10	9.64E+09
Xe-133m	4.92E+08	2.80E+08
Xe-135	3.45E+09	2.36E+09
Xe-135m	3.42E+09	1.29E+08
Xe-138	1.31E+10	0.00E+00
Total	4.86E+10	1.28E+10

CHAPTER 13

ACCIDENT ANALYSES



AAI-PSAR-13 (NP) Rev 0

Page 13-26

Table 13-9: Results of the offsite 24-hour dose consequence assessment at 150 m

Parameter	Value	Unit
TEDE (24 hr max)	0.34	rem

For a receptor 150 m from the release point the TEDE for 24 hours is 0.34 rem which is well below the regulatory maximum of 1 rem.

13.3.2 Insertion of Excess Reactivity

13.3.2.1 Rapid Inadvertent Insertion of a Portion of All Excess Reactivity Loaded into the Reactor

This accident is bounded by the analysis discussed in Section 13.3.2.3, the rapid insertion of a fuel assembly into a vacancy in the core at the most reactive position. This section will be further developed in the FSAR submittal to include a topical treatment of potential initiating events.

13.3.2.2 Rapid Removal of the Most Reactive Control Rods

The rapid removal of any control rods from the VIPR core is not considered plausible because the reactor operates at ambient pressures and low temperatures. Additionally, the VIPR is not designed for pulsed operation and no power or temperature excursions, apart from the other accidents discussed, are anticipated.

13.3.2.3 Rapid Insertion of a Fuel Element into a Vacancy in the Core at the Most Reactive Position

A rapid insertion of a fuel assembly into a vacancy in the core is postulated to occur from a fuel assembly, perched above the most reactive position in the VIPR core, falling into its fully seated position. When this step insertion of reactivity occurs while the VIPR is at full power, excess reactivity causes the reactor to enter a supercritical configuration and begin a rapid power excursion. Such an excursion consequently increases the temperature of the fuel, cladding, and primary coolant which may approach regulatory and safety limits.

Should a fuel assembly rapidly insert into the core, the transient is terminated by the reactor overpower trip of the Reactor Protection System. The reactor is tripped early enough during this transient that departure from nucleate boiling does not occur and the PCS is able to remove the heat from the fuel assembly. With the reactor tripped, the facility returns to a stable condition.

Credit is taken for the low thermal power of the VIPR, the relatively low primary coolant temperature and pressure, and the large mass of coolant present in the system in overturning the power excursion and mitigating its effects.

13.3.2.3.1 Initial Conditions

In the analysis of this event, the reactor is assumed to be in the hot, full power condition described in **Table** 13-1. In this state all core components are at their maximum postulated steady-state temperatures, minimizing the margin to their safety and regulatory limits.

The perched fuel assembly is elevated 8.00 cm above its nominal position, corresponding to a reactivity insertion of 0.75 \$ when it is fully lowered in the core.



AAI-PSAR-13 (NP) Rev 0

Page 13-27

It is additionally assumed that this event occurs at the beginning of the first fuel cycle, when the excess reactivity of the system is at a maximum. The control rods begin inserted into the core at the position required for the reactor to initially achieve criticality with the perched fuel assembly in its suboptimal position partially removed from the core, which maximizes the power density throughout the evolution of the transient and, consequently, the local temperatures of core components. This combination of conditions places the greatest limitations on several safety and regulatory limits, including the fuel centerline and cladding temperatures. Because it is determined that all fuel cladding integrity is maintained from accident initiation to the termination of the transient, no assumptions about radiation source terms were made.

13.3.2.3.2 Identification of Causes

The rapid insertion of a fuel assembly into the most reactive vacancy in the VIPR core can occur as a result of human or administrative error during refueling operations.

13.3.2.3.3 Sequence of Events and Systems Operation

The sequence of events for the rapid insertion of a fuel assembly into a vacancy in the core is as follows:

- 00:00:00.00: The perched fuel assembly falls from its elevated position into the VIPR core; this
 is assumed to occur as an instantaneous step insertion of reactivity, rather than a rapid ramp
 insertion of reactivity.
- 00:00:00.10: Reactor overpower signal occurs.
- 00:00:01.10: Reactor trip signal triggers and control rods begin to insert. Reactor power begins to decrease.
- 00:00:01.22: Hot pin cladding temperature reaches its maximum and begins to decrease.
- 00:00:01.40: Hot pin fuel centerline temperature reaches its maximum and begins to decrease.
- 00:00:01.49: Coolant temperature reaches its maximum and begins to decrease. Fuel and cladding temperatures in the average fuel pin and the hot fuel pin continue to decrease until the reactor reaches a stable shutdown condition.
- 00:00:01.68: Control rods fully inserted.

It is assumed in this scenario that the overpower sensors and reactor scram circuitry are operational. No other plant systems, reactor protection systems, or operator actions are required in the mitigation of this event.

13.3.2.3.4 <u>Damage to Equipment</u>

No damage is anticipated to occur in the fuel, any equipment or components, the reactor building, or radioactive material barriers over the course of this accident. The reactor is tripped sufficiently early during the transient to preclude any damage to it or any related systems.

CHAPTER 13 ACCIDENT ANALYSES

13.3.2.3.5 Core and System Performance

The insertion of a fuel assembly into the most reactive vacancy in the VIPR core represents the largest possible step insertion of reactivity into the VIPR. With the reactor already in a critical configuration, the reactivity insertion initiates an immediate power excursion, accompanied by the corresponding rise in the fuel, cladding, and coolant temperatures. The temperature-dependent reactivity feedback effects in the fuel and coolant partially offset the reactivity added by the full insertion of the perched fuel assembly, until the reactor overpower signal triggers and scrams the reactor after the assumed time delay. The maximum temperatures in the fuel and cladding occur shortly after the control rods begin to drop, as their temperatures immediately begin to fall as reactor power decreases. The maximum heat flux, resulting in the minimum departure from nucleate boiling ratio (DNBR), occurs around this time. The fuel, cladding, and coolant all reach approximately the same temperature following the accident after the reactor shutdown.

The predicted temperatures in the hot channel over the course of the accident are plotted against the reactor power in Figure 13-2, Figure 13-3, and Figure 13-4. The International Atomic Energy Agency (IAEA) gives a nominal uranium dioxide melting temperature of 3120 K (2846.85 °C). This analysis conservatively used 2804 °C, accounting for Nuclear Regulatory Commission (NRC)-accepted adjustments for burnup (-5 C for every 10 GWd/MTU burnup per NUREG/CR-7024), as the hot pin fuel centerline safety limit temperature based on this higher IAEA melting temperature.

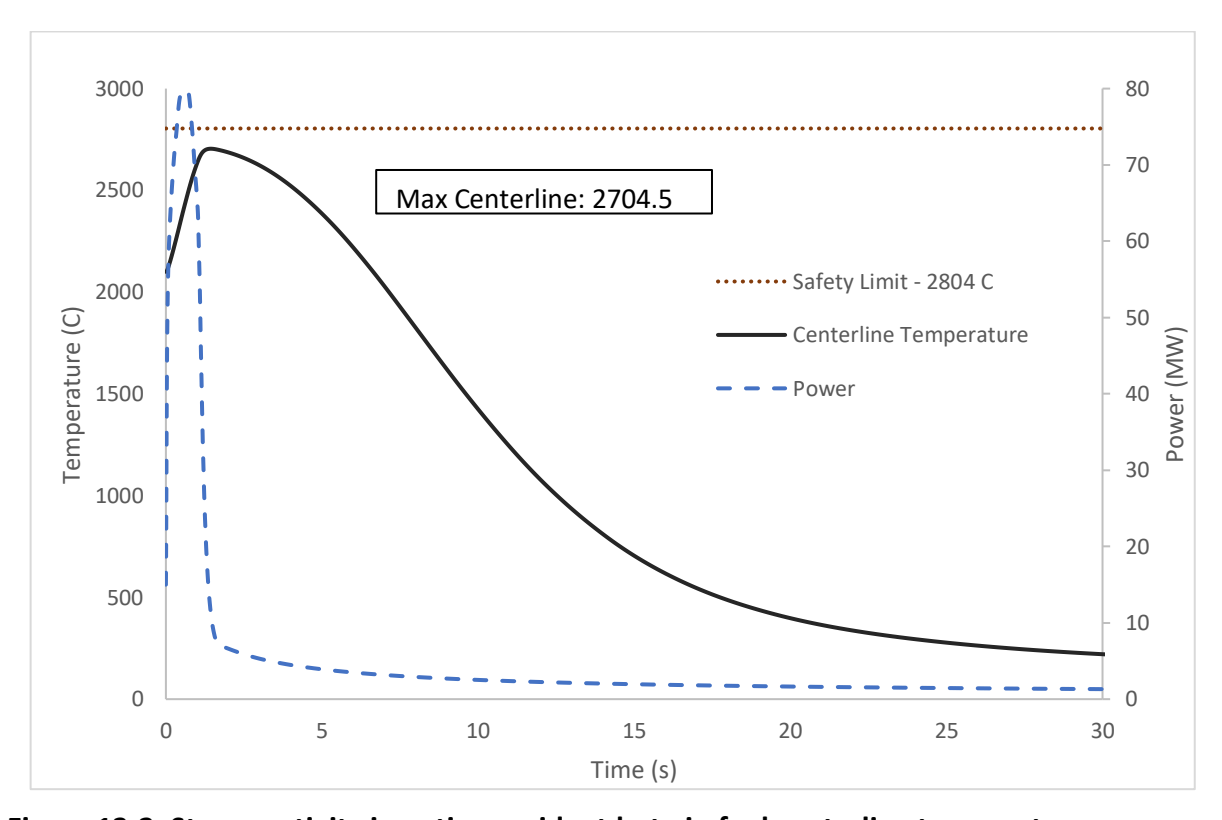


Figure 13-2: Step reactivity insertion accident hot pin fuel centerline temperature response



CHAPTER 13 ACCIDENT ANALYSES

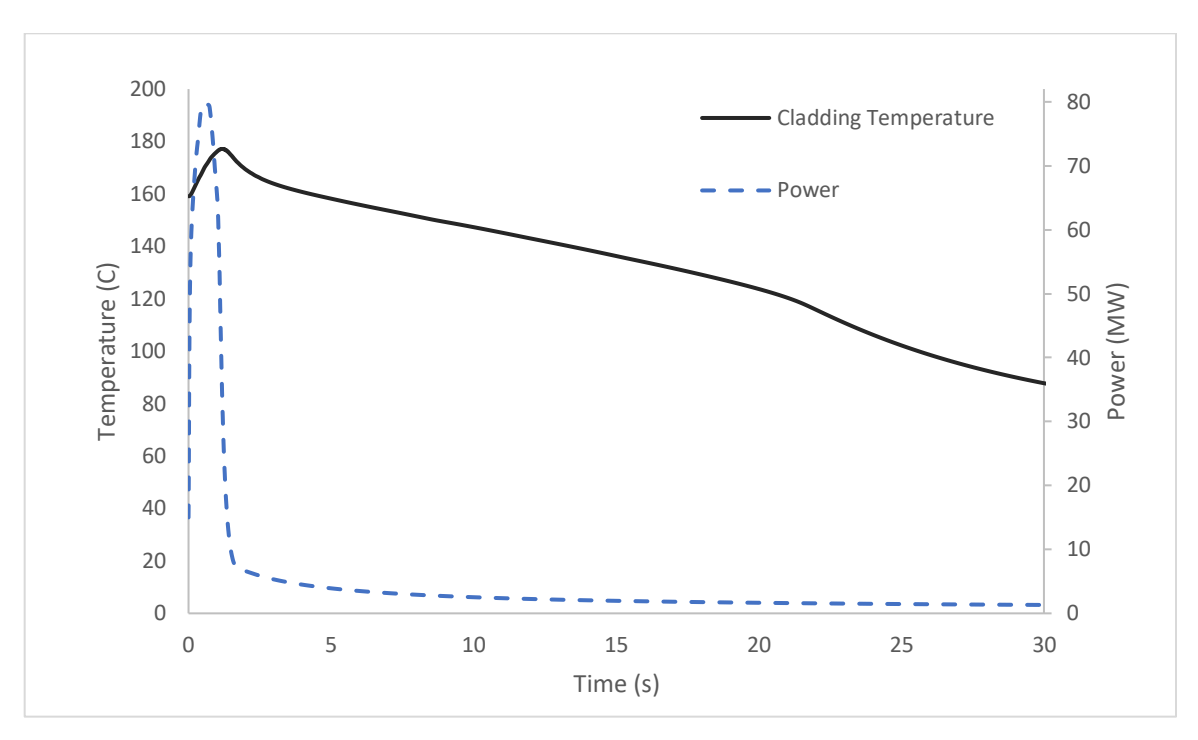


Figure 13-3: Step reactivity insertion accident hot pin cladding temperature response

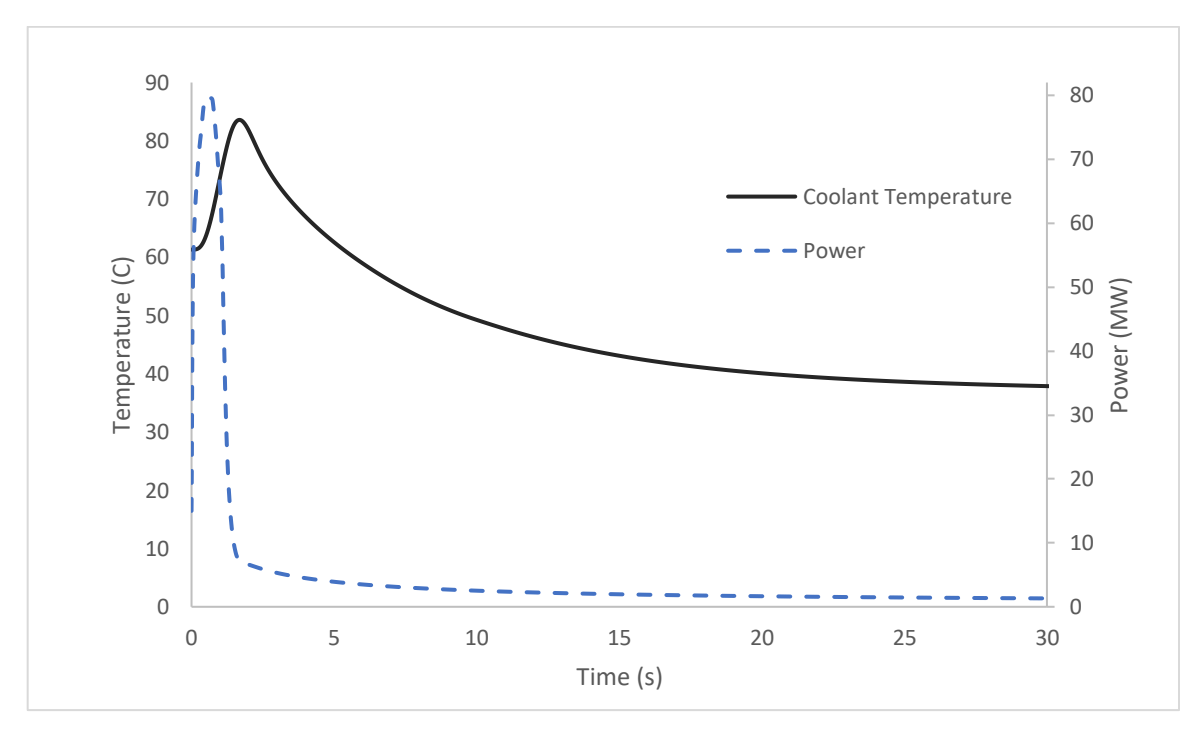


Figure 13-4: Step reactivity insertion accident bulk coolant core exit temperature response





Page 13-30

Table 13-10: Step reactivity insertion accident output parameters

Parameter	Value	Unit
Power (Maximum)	79.5	MW
Hot Pin Fuel Centerline (Maximum)	2704.5	°C
Hot Pin Cladding (Maximum)	177	°C
Coolant Outlet Temperature (Maximum)	84.0	°C
DNBR (Minimum)	1.6	

13.3.2.3.6 Barrier Performance

Because the maximum temperatures reached in the hot pin fuel centerline and cladding each remain below their respective safety limits throughout the accident, it is assumed that no fuel pin will violate either limit during the accident, and the integrity of all cladding is assured. Furthermore, as the maximum expected heat flux is less than the minimum critical heat flux, no departure from nucleate boiling is anticipated, and no cladding degradation from oxidation is anticipated.

13.3.2.3.7 Radiological Consequences

As all radiological barriers are anticipated to remain intact, and all biological shielding will remain intact and undamaged, there is no radiological release anticipated from this accident.

13.3.2.4 Ramp Insertion of Reactivity by Drive Motion of the Most Reactive Control Rods

A ramp insertion of reactivity is caused by the continuous removal of the most reactive control rods from the VIPR in an uncontrolled fashion, without regard for reactor power, neutron flux levels, or temperatures within the core. When such a withdrawal occurs while the VIPR is at full power, excess reactivity causes the reactor to enter a supercritical configuration and begin a power excursion. Such an excursion consequently increases the temperature of the fuel, cladding, and primary coolant which may approach regulatory and safety limits.

Should a rod withdrawal accident occur, the transient is terminated by the reactor overpower trip of the Reactor Power System. Should an uncontrolled control rod assembly withdrawal occur at power, the reactor is tripped early enough during the transient that departure from nucleate boiling does not occur and the ability of the PCS to remove heat from the fuel rods is not reduced. With the reactor tripped, the facility returns to a stable condition.

Credit is taken for the low thermal power of the VIPR, the relatively low primary coolant temperature and pressure, and the large mass of coolant present in the system in overturning the power excursion and mitigating its effects.

13.3.2.4.1 Initial Conditions

In the analysis of this event, the reactor is assumed to be in the hot, full power condition described in **Table 13-1**. In this state all core components are at their maximum postulated steady-state



AAI-PSAR-13 (NP) Rev 0

Page 13-31

temperatures, minimizing the margin to their safety and regulatory limits. It is additionally assumed that this event occurs at the beginning of the first fuel cycle, when the excess reactivity of the system is at a maximum. The control rods begin inserted into the core at the position required for the reactor to initially achieve criticality, which maximizes the power density throughout the evolution of the transient and, consequently, the local temperatures of core components. This combination of conditions places the greatest limitations on several safety and regulatory limits, including the fuel centerline and cladding temperatures. Because it is determined that all fuel cladding integrity is maintained from accident initiation to the termination of the transient, no assumptions about radiation source terms were made.

13.3.2.4.2 Identification of Causes

A ramp insertion of reactivity resulting from the removal of the VIPR control rods can occur as a result of operator error or malfunction of the control rod drive mechanism components or Instrumentation and Control rod control systems.

13.3.2.4.3 Sequence of Events and Systems Operation

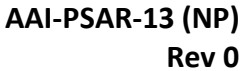
The sequence of events for a ramp insertion of reactivity caused by the drive motion of the control rods is as follows:

- 00:00:00.00: The control rod drive malfunction causes the most reactive control rods to begin withdrawing from the core at the maximum rate.
- 00:00:00.78: Reactor overpower signal occurs.
- 00:00:01.78: Reactor trip signal triggers and control rods begin to insert. Reactor power begins to decrease.
- 00:00:03.05: Hot pin cladding temperature reaches its maximum and begins to decrease.
- 00:00:03.11: Hot pin fuel centerline temperature reaches its maximum and begins to decrease.
- 00:00:03.60: Control rods fully inserted.
- 00:00:03.67: Coolant temperature reaches its maximum and begins to decrease. Fuel and cladding temperatures in the average fuel pin and the hot fuel pin continue to decrease until the reactor reaches a stable shutdown condition.

It is assumed in this scenario that the overpower sensors and reactor scram circuitry are operational. No other plant systems, reactor protection systems, or operator actions are required in the mitigation of this event.

13.3.2.4.4 Damage to Equipment

No damage is anticipated to occur in the fuel, any equipment or components, the reactor building, or radioactive material barriers over the course of this accident. The reactor is tripped sufficiently early during the transient to preclude any damage to it or any related systems.







13.3.2.4.5 Core and System Performance

The removal of the most reactive control rods at the maximum rate represents the largest possible ramp insertion of reactivity into the VIPR. With the reactor already in a critical configuration, the removal of the control rods initiates an immediate power excursion, accompanied by the corresponding rise in the fuel, cladding, and coolant temperatures. The temperature-dependent reactivity feedback effects in the fuel and coolant partially offset the reactivity added by the removal of the control rods, until the reactor overpower signal triggers and scrams the reactor after the assumed time delay.

It is assumed there is still offsite power and the PCS pumps are operating at the limiting safety system setting conditions of [] PROP. All control rod groups are assumed to fall back into the core under the force of gravity. The maximum temperatures in the fuel and cladding occur shortly after the control rods drop, as their temperatures immediately begin to fall as reactor power decreases.

The predicted temperatures in the hot channel over the course of the accident are plotted against the reactor power in **Figure** 13-5, **Figure** 13-6, and **Figure** 13-7. The hot pin fuel centerline temperature does not exceed the established safety limit of 2804 °C.

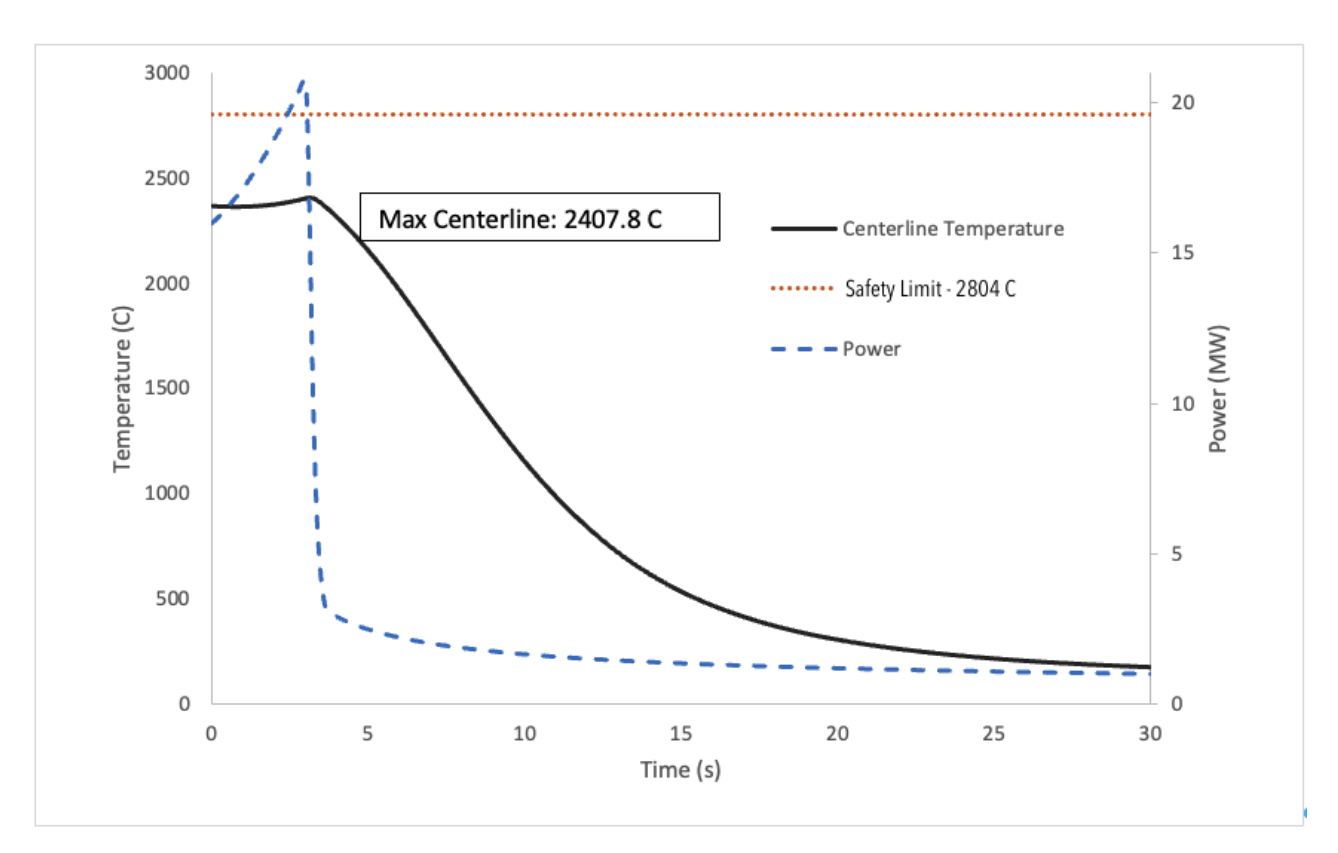
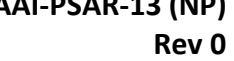


Figure 13-5: Ramp reactivity insertion accident hot pin fuel centerline temperature response





CHAPTER 13 ACCIDENT ANALYSES

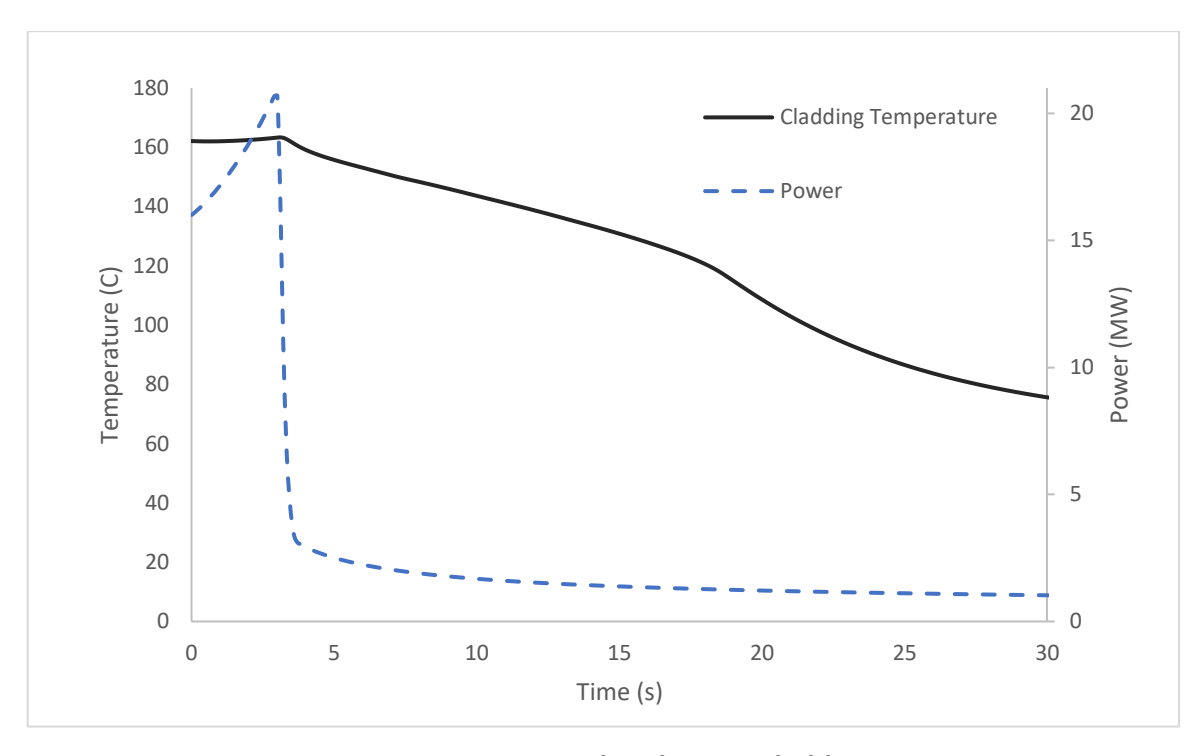


Figure 13-6: Ramp reactivity insertion accident hot pin cladding temperature response

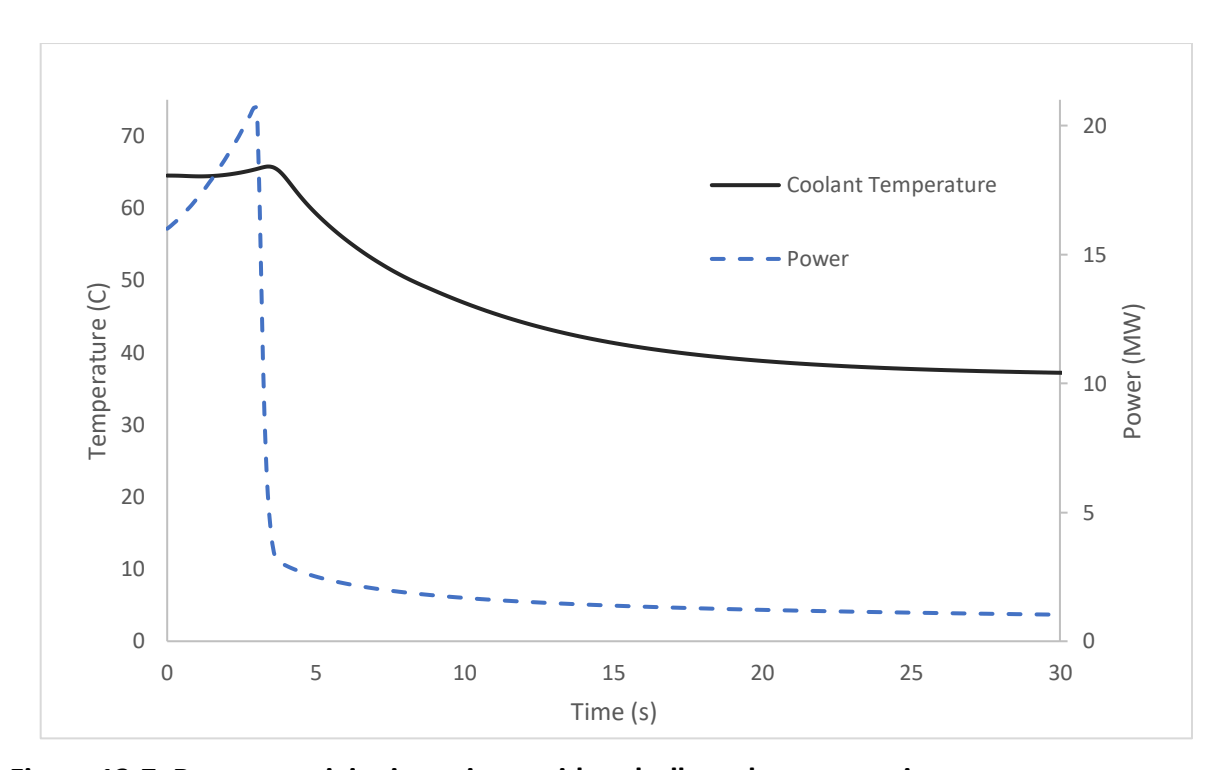


Figure 13-7: Ramp reactivity insertion accident bulk coolant core exit temperature response



Table 13-11: Ramp reactivity insertion accident output parameters

Parameter	Value	Unit
Power (Maximum)	20.7	MW
Hot Pin Fuel Centerline	2407.8	°C
Hot Pin Cladding (Surface)	163.3	°C
Coolant Outlet Temperature (Maximum)	65.75	°C
DNBR (Minimum)	2.72	

13.3.2.4.6 Barrier Performance

Because the maximum temperatures reached in the hot pin fuel centerline and cladding each remain below their respective safety limits throughout the accident, it is assumed that no fuel pin will violate either limit during the accident, and the integrity of all cladding is assured. Furthermore, as the maximum expected heat flux is less than the minimum critical heat flux no departure from nucleate boiling is anticipated, and no cladding degradation from oxidation is anticipated.

13.3.2.4.7 Radiological Consequences

As all radiological barriers are anticipated to remain intact, and all biological shielding will remain intact and undamaged, there is no radiological release anticipated from this accident.

13.3.2.5 Failure of an Experiment that Inserts Excess Reactivity

This accident is bounded by the analysis discussed in Section 13.3.2.3, the rapid insertion of a fuel assembly into a vacancy in the core at the most reactive position.

13.3.2.6 Rapid Increase in Reactivity as a Result of a Change in Operating Parameters

This accident is bounded by the analysis discussed in Section 13.3.2.3, the rapid insertion of a fuel assembly into a vacancy in the core at the most reactive position.

13.3.3 Loss of Coolant

13.3.3.1 Failure of a Component in the Primary Coolant Loop

This accident is bounded by the analysis discussed in Section 13.3.3.4, a failure of the PCS boundary. This section will be further developed in the FSAR submittal to include a topical treatment of potential initiating events.

13.3.3.2 Failure in the Chemical and Volume Control System

This accident is bounded by the analysis discussed in Section 13.3.3.4, a failure of the PCS boundary. This section will be further developed in the FSAR submittal to include a topical treatment of potential initiating events.



AAI-PSAR-13 (NP) Rev 0

Page 13-35

13.3.3.3 Failure of an Experimental Facility

This accident is bounded by the analysis discussed in Section 13.3.3.4, a failure of the PCS boundary. This section will be further developed in the FSAR submittal to include a topical treatment of potential initiating events.

13.3.3.4 Failure of the Primary Coolant Boundary

The bounding loss of coolant event is caused by the failure of the PCS boundary, resulting in a rapid, large-scale loss of coolant accident. Specifically, a large piping break, such as a double guillotine break, is assumed to occur in the cold leg of the primary coolant loop inside of the PCS pump and heat exchanger cavity in the auxiliary module. This location is considered the most limiting because of the low elevation of the break and of all connecting piping relative to the reactor pool. The equilibrium water level established between the reactor pool and auxiliary module cavity leaves several meters of coolant remaining above the VIPR core. The principal concerns in a loss of coolant accident are dissipation of decay heat from the fuel and shielding from radiation emitted from the core with the volume of coolant remaining in the reactor pool.

Should a loss of coolant occur, the reactor is shut down by the reactor pool low level trip by the Reactor Protection System. Credit is taken for the low thermal power of the VIPR, the relatively low primary coolant temperature and pressure, the large mass of coolant present in the system, and the volume of the auxiliary module cavity in mitigating the effects of the accident.

13.3.3.4.1 Initial Conditions

In the analysis of this event, the reactor is assumed to be in the hot, full power condition described in **Table** 13-1. In this state all core components are at their maximum postulated steady-state temperatures, minimizing the margin to their safety and regulatory limits. It is additionally assumed that this event occurs at the beginning of the first fuel cycle, when the excess reactivity of the system is at a maximum. The control rods begin inserted into the core at the position required for the reactor to initially achieve criticality, which maximizes the power density throughout the evolution of the transient and, consequently, the local temperatures of core components. This combination of conditions places the greatest limitations on several safety and regulatory limits, including the fuel centerline and cladding temperatures. Because it is determined that all fuel cladding integrity is maintained from accident initiation to the termination of the transient, no assumptions about radiation source terms were made.

13.3.3.4.2 Identification of Causes

The loss of coolant occurs as a result of a failure of the PCS boundary.

13.3.3.4.3 <u>Sequence of Events and Systems Operation</u>

The loss of coolant accident can occur as a malfunction of the PCS boundary.

 00:00:00.00: The PCS boundary fails, allowing primary coolant to drain into the auxiliary module cavity. Primary coolant velocity through the core begins to slow. Reactor power begins to decrease as temperatures in the VIPR core increase. Hot pin fuel centerline and cladding temperature begins to decrease.



AAI-PSAR-13 (NP) Rev 0

Page 13-36

- 00:00:00.13: Low primary coolant flow signal occurs.
- 00:00:00.40: Coolant flow reverses to downward flow through the core.
- 00:00:01.13: Reactor trip signal triggers and control rods begin to insert. Reactor power begins to decrease more rapidly.
- 00:00:01.70: Control rods fully inserted.
- 00:00:02.30: Cladding temperature in the hot pin reaches its minimum.
- 00:03:35.00: Reactor pool drained to equilibrium level.

It is assumed in this scenario that the overpower sensors and reactor scram circuitry are operational. No other plant systems, reactor protection systems, or operator actions are required in the mitigation of this event.

13.3.3.4.4 <u>Damage to Equipment</u>

Submersion of the primary coolant pumps, heat exchanger, and related systems and components contained in the auxiliary module cavity is expected to result in damage to these systems and components. No additional damage is anticipated to occur in the fuel, the reactor building, or radioactive material barriers over the course of this accident.

13.3.3.4.5 Core and System Performance

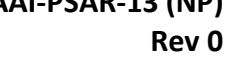
The failure of the PCS boundary represents the most severe loss of coolant accident in the VIPR. Because the accident occurs on the PCS cold leg before the core, forced convective flow is instantaneously lost and the coolant velocity begins to decrease. With the reactor operating at full power, reduced flow increases the residence time of coolant in the core, which increases coolant temperatures through the core. The temperature-dependent reactivity feedback effect of coolant decreases the power of the reactor, until the low primary coolant flow signal triggers and scrams the reactor after the assumed time delay.

All control rod groups are assumed to fall into the core under the force of gravity.

Around this time, the coolant draining into the auxiliary module cavity causes a flow reversal in the VIPR core, with downward velocities cooling the cladding and reducing the core coolant temperature to the pool average temperature. The pool drains through the cold leg of the PCS until the water levels in the cavity and pool are equal. At this point the accident sequence of events is considered finished; however, owing to the reduced volume of coolant remaining in the reactor pool, more detailed analysis of the long-term behavior of the system is given.

The maximum temperatures in the fuel and cladding occur at the beginning of the accident during the flow reversal. Their temperatures immediately begin to fall as reactor power decreases in response to the rising coolant temperatures and the reactor scram.

The predicted temperatures in the hot channel over the course of the accident are plotted against the reactor power in **Figure 13-8**, **Figure 13-9**, and **Figure 13-10**.





CHAPTER 13 ACCIDENT ANALYSES

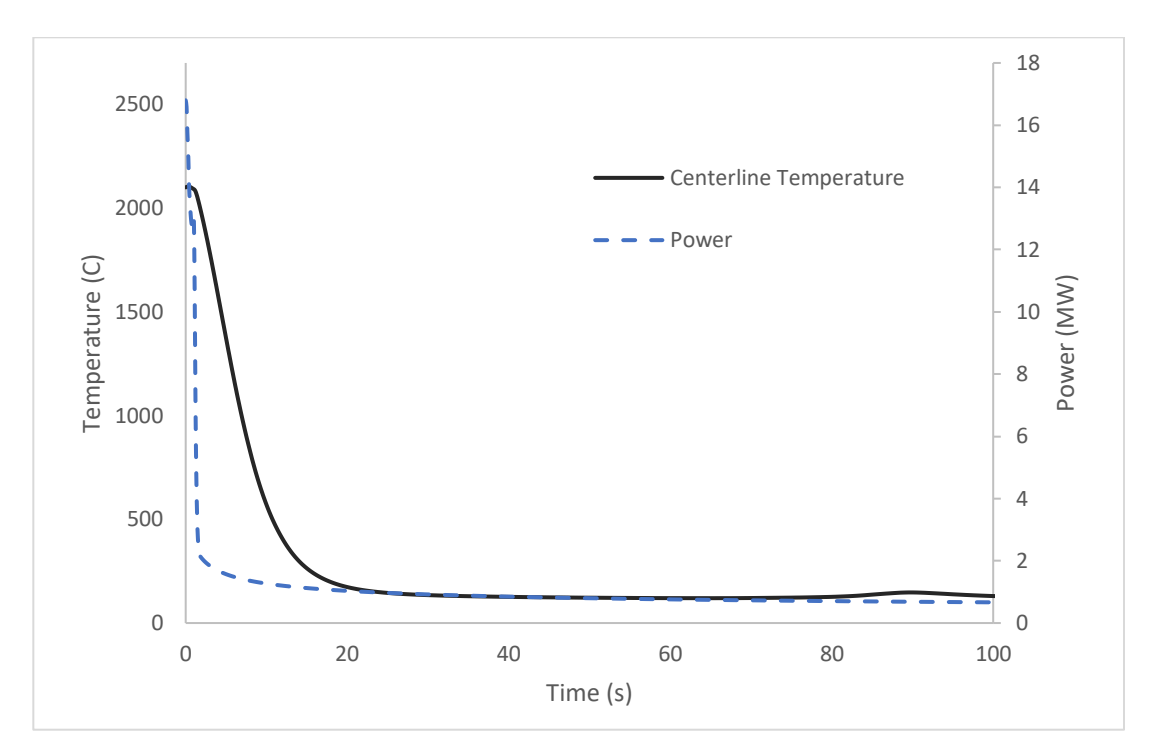


Figure 13-8: Loss of coolant accident hot pin fuel centerline temperature response

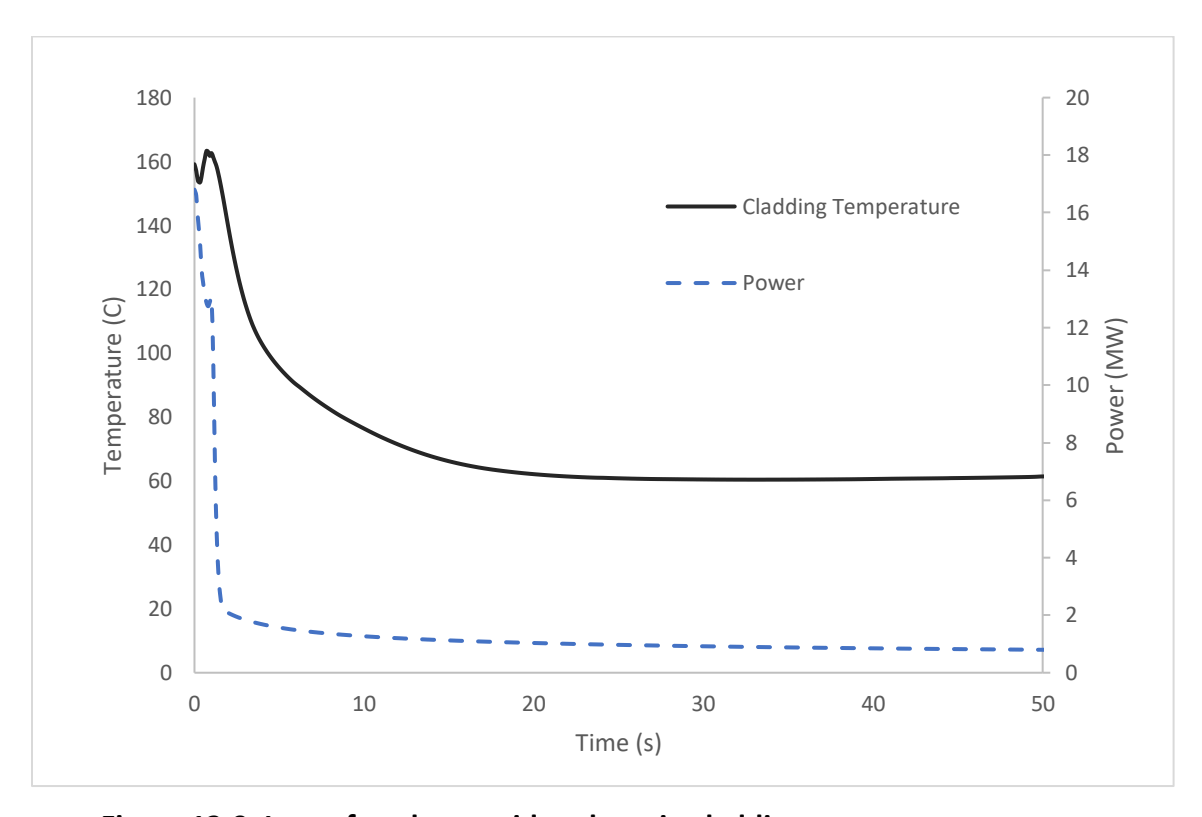
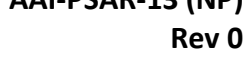
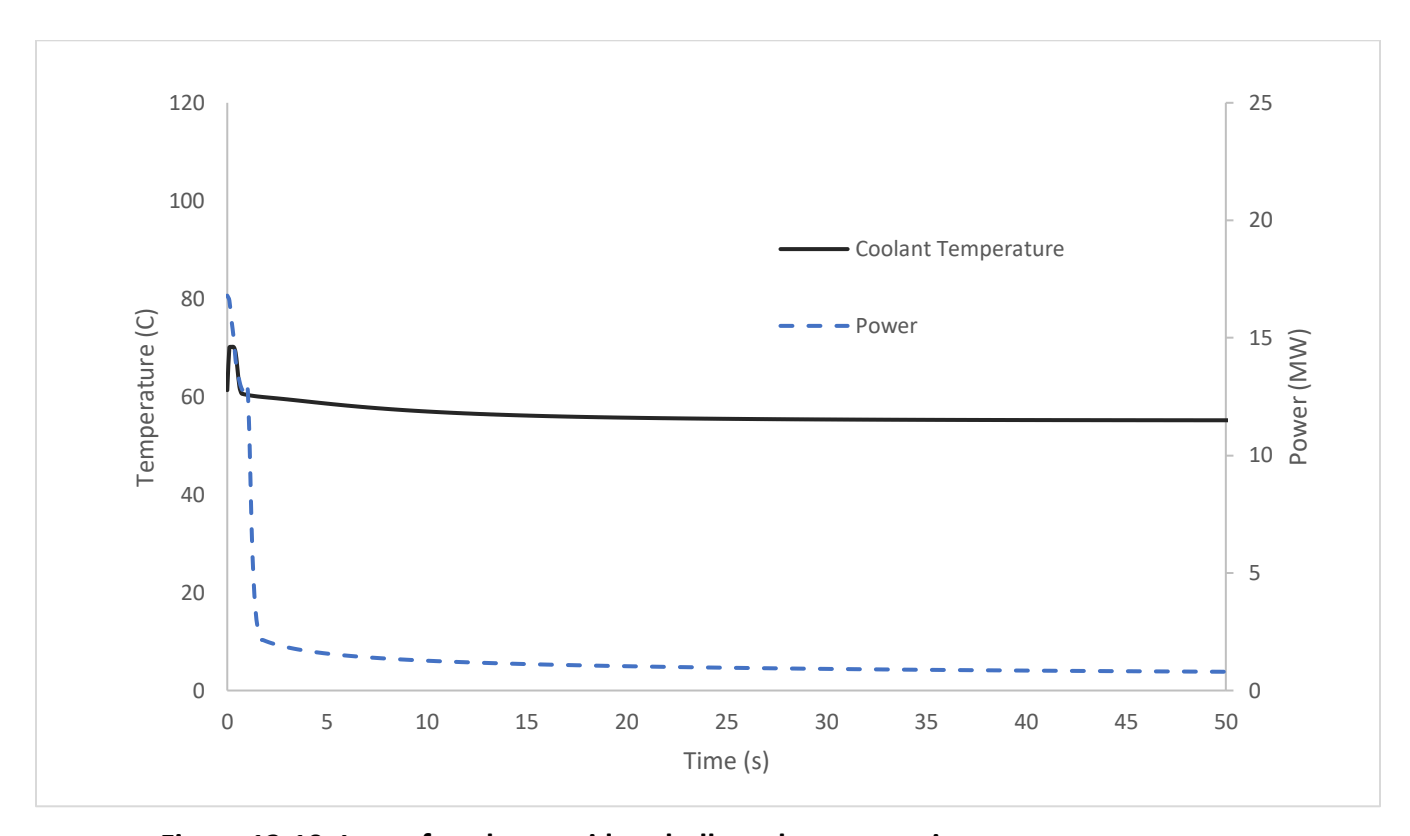


Figure 13-9: Loss of coolant accident hot pin cladding temperature response





ACCIDENT ANALYSES Page 13-38



CHAPTER 13

Figure 13-10: Loss of coolant accident bulk coolant core exit temperature response

The flow suffers from instability during the transition to reverse flow. The velocity of the coolant downward through the core during the accident, shown in Figure 13-11, Figure 13-11 slowly decreases as the auxiliary pit reaches equilibrium. When the coolant in the auxiliary module cavity and reactor pool reaches its equilibrium level, natural convection is established to cool the reactor core.





CHAPTER 13 ACCIDENT ANALYSES

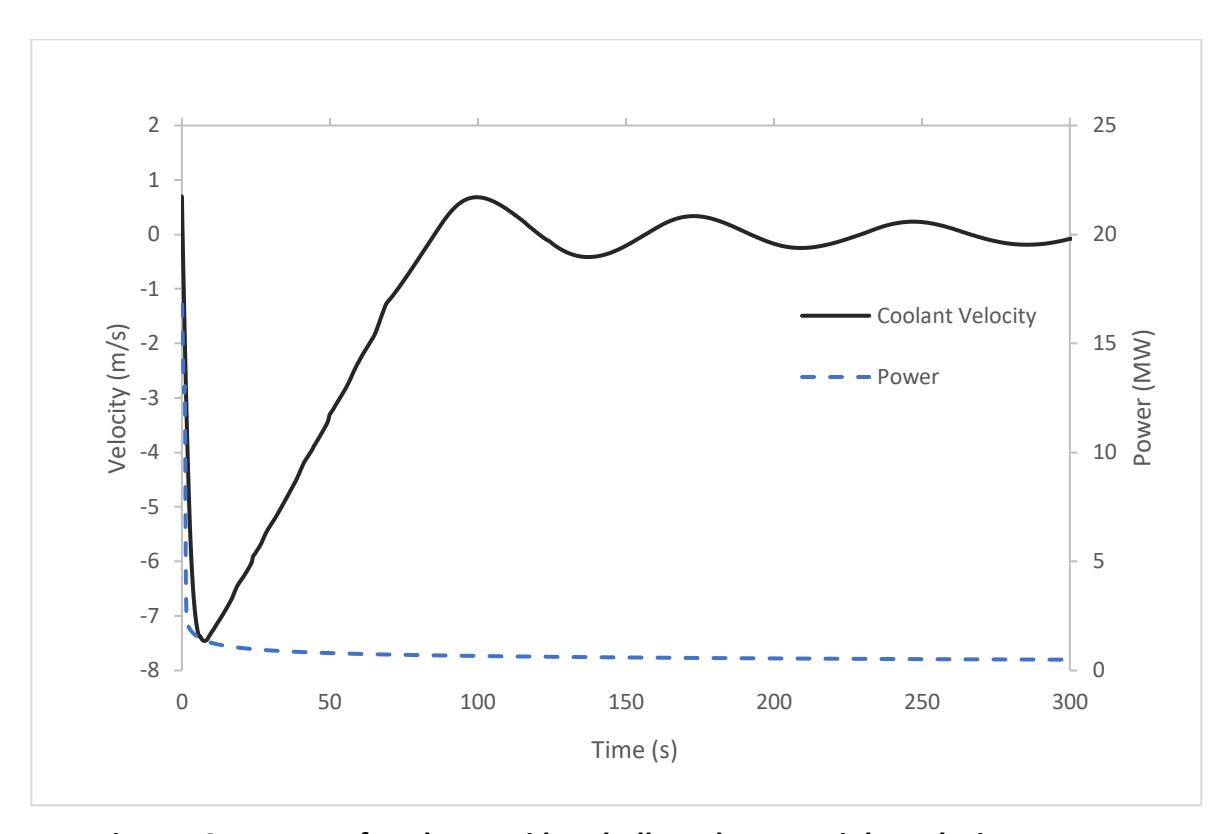


Figure 13-11: Loss of coolant accident bulk coolant core inlet velocity response

The sporadic localized boiling becomes less frequent as the decay heat and temperature of the fuel each decrease. The fuel, cladding, and coolant all reach approximately the same temperature following the accident and reactor shutdown. With the cessation of heat removal from the secondary coolant system, all temperatures within the reactor module slowly increase without bound following the accident due to the decay heat. The long-term behavior of the system is of interest in the analysis of this accident, owing to the decreased volume of coolant available to absorb the decay heat from the fuel. The predicted temperatures of the hot pin fuel centerline, hot pin cladding, and coolant over 72 hours following the accident are shown in Figure 13-12. The majority of the energy released over the course of the accident occurs before the reactor is shut down; because of the decay heat produced in the fuel, however, the amount of energy deposited in the system steadily increases over the 72 hours after the accident occurs.



CHAPTER 13 ACCIDENT ANALYSES

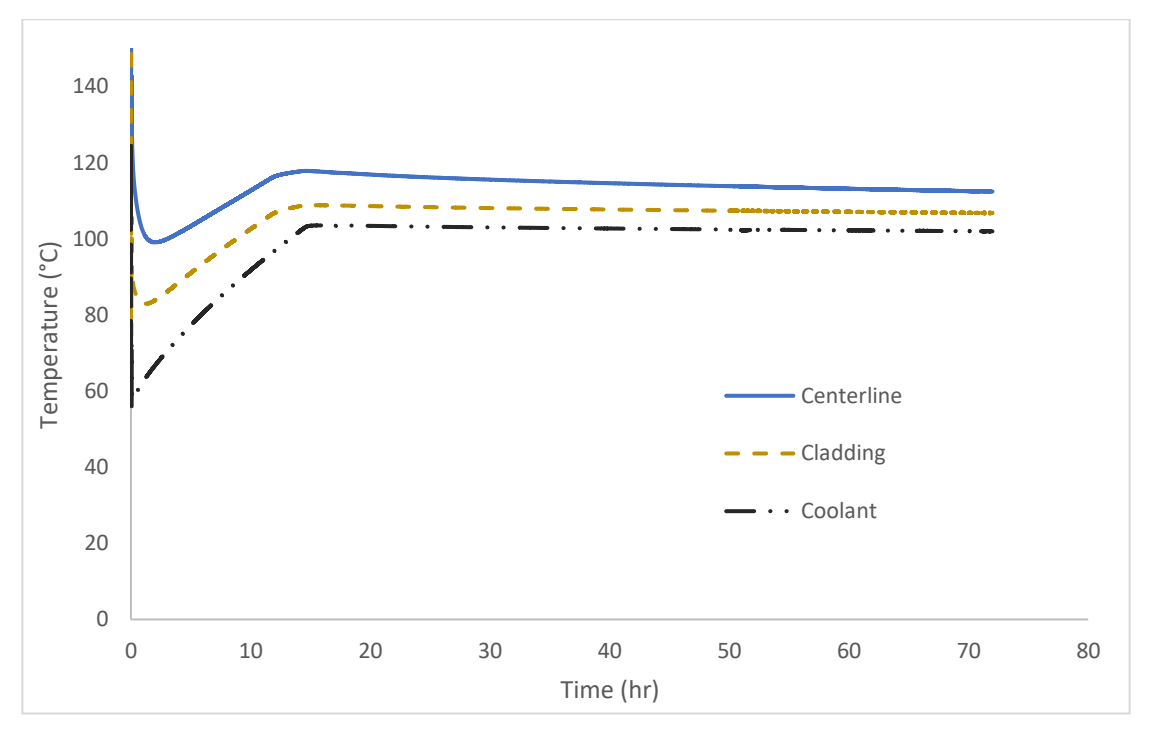


Figure 13-12: Hot pin and bulk coolant temperatures following a loss of coolant accident

Table 13-12: Loss of coolant accident output parameters

Parameter	Value	Unit
Power (Maximum)	16.80	MW
Hot Pin Fuel Centerline (Maximum)	2377.7	°C
Hot Pin Cladding (Maximum)	164	°C
Coolant Outlet Temperature (Maximum)	118.1	°C
Equilibrium Coolant Depth Above Core	4.55	m

13.3.3.4.6 Barrier Performance

Because the maximum temperatures reached in the hot pin fuel centerline and cladding each remain below their respective safety limits throughout the accident, it is assumed that no fuel pin will violate either limit during the accident, and the integrity of all cladding is assured. The impact of vapor rate and time duration on oxidation on the cladding will be further developed in the FSAR.

13.3.3.4.7 Radiological Consequences

As all radiological barriers are anticipated to remain intact, there is no radiological release anticipated from this accident. However, the decreased volume of water above the VIPR core results in a decrease



AAI-PSAR-13 (NP) Rev 0

Page 13-41

in its efficacy as a biological shield. The flux of neutrons and photons produced by the fuel was determined by stochastic simulation of the core in MCNP6.2. The dose rate, conservatively evaluated at a pool depth of 4.5 meters, was calculated using particle fluence to dose conversion factors from ANSI/ANS-6.1.1-2020, "Photon and Neutron Fluence-To-Dose Conversion Coefficients." 200 seconds after shutdown, approximately the time when the reactor pool is drained to 4.5 m, the anticipated dose at the pool surface is 406 mrem/h; after 3 days the dose falls to 59 mrem/h.

13.3.4 Loss of Coolant Flow

13.3.4.1 Loss of Electrical Power

This accident is bounded by the analysis discussed in Section 13.3.4.2, the failure of a component of the PCS. This section will be further developed in the FSAR submittal to include a topical treatment of potential initiating events.

13.3.4.2 Failure of a Component in the Primary Coolant System

The bounding loss of coolant flow event is caused by the failure of a component of the PCS, such that forced convection of coolant through the VIPR core immediately ceases. Operation of the VIPR at full power without the appropriate coolant flow, as occurs in the period of time before the reactor is automatically shut down, increases the temperature of the fuel, cladding, and primary coolant which may approach regulatory and safety limits.

This accident is considered separately from the loss of coolant accidents discussed in Section 13.3.3; as such, the integrity of the PCS boundary is maintained and no coolant loss from the PCS is considered.

Should a loss of coolant flow occur, the reactor is shut down by the low primary coolant flow trip or reactor inlet temperature trip by the reactor protection system, whichever setpoint is reached first. The reactor is tripped early enough during the transient that departure from nucleate boiling does not occur in the bulk of the fuel and the PCS is able to remove heat from the fuel rods. The hot pins in the reactor do experience film boiling but the cladding temperature does not surpass the safety limit. With the reactor tripped, the facility returns to a stable condition.

Credit is taken for the low thermal power of the VIPR, the relatively low primary coolant temperature and pressure, and the large mass of coolant present in the system in mitigating the effects of the accident.

13.3.4.2.1 Initial Conditions

In the analysis of this event, the reactor is assumed to be in the hot, full power condition described in **Table** 13-1. In this state all core components are at their maximum postulated steady-state temperatures, minimizing the margin to their safety and regulatory limits. It is additionally assumed that this event occurs at the beginning of the first fuel cycle, when the excess reactivity of the system is at a maximum. The control rods begin inserted into the core at the position required for the reactor to initially achieve criticality, which maximizes the power density throughout the evolution of the transient and, consequently, the local temperatures of core components. This combination of conditions places the greatest limitations on several safety and regulatory limits, including the fuel centerline and cladding temperatures. Because it is determined that all fuel



AAI-PSAR-13 (NP) Rev 0

Page 13-42

cladding integrity is maintained from accident initiation to the termination of the transient, no assumptions about radiation source terms were made.

13.3.4.2.2 Identification of Causes

The loss of coolant flow as a result of a failure of a component in the PCS can occur as a result of operator error or malfunction of the PCS components.

13.3.4.2.3 Sequence of Events and Systems Operation

The sequence of events for a loss of coolant flow is as follows:

- 00:00:00.00: A component of the PCS fails, causing forced convection of the primary coolant to cease. Reactor power begins to decrease as rising coolant temperatures enhance negative temperature feedback mechanisms. Hot pin fuel centerline and cladding temperature begins to decrease.
- 00:00:00.13: Low primary coolant flow signal occurs.
- 00:00:01.13: Reactor trip signal triggers and control rods begin to insert. Reactor power begins to decrease more rapidly.
- 00:00:01.70: Control rods fully inserted.
- 00:00:01.90: Coolant temperature reaches its maximum and begins to decrease.
- 00:00:05.90: Fuel and cladding temperatures in the average fuel pin and the hot fuel pin continue to decrease until the reactor reaches a stable shutdown condition.

It is assumed in this scenario that the primary coolant flow sensors and reactor scram circuitry are operational. No other plant systems, reactor protection systems, or operator actions are required in the mitigation of this event.

13.3.4.2.4 Damage to Equipment

No damage is anticipated to occur in the fuel, any equipment or components, the reactor building, or radioactive material barriers over the course of this accident. The reactor is tripped sufficiently early during the transient to preclude any damage to it or any related systems.

13.3.4.2.5 Core and System Performance

The failure of a component of the PCS represents the most severe loss of coolant flow accident in the VIPR. With the reactor operating at full power the loss of forced flow results increases the residence time of coolant in the core, which increases coolant temperatures through the core. The temperature-dependent reactivity feedback effect of coolant decreases the power of the reactor, until the low primary coolant flow signal triggers and scrams the reactor after the assumed time delay. The temperature of the coolant rises to a maximum determined by the decreasing decay heat and temperature of the fuel and cladding, after which it falls to its shutdown temperature.

No primary coolant pump coastdown is assumed, although the momentum of the fluid results in a gradual decrease in flow velocity rather than an instantaneous drop.







CHAPTER 13 ACCIDENT ANALYSES

All control rod groups are assumed to fall into the core under the force of gravity.

The maximum temperatures in the fuel and cladding occur at the beginning of the accident, as their temperatures immediately begin to fall as reactor power decreases in response to the rising coolant temperatures.

The predicted temperatures in the hot channel over the course of the accident are plotted against the reactor power in Figure 13-13, Figure 13-14, and Figure 13-15. Initial temperature fluctuations observed in both the cladding and coolant are consistent with expected transient thermal-hydraulic behavior, including the onset of film boiling in high-power regions. While a transition to film boiling temporarily reduces heat transfer efficiency, peak cladding temperatures remain within established safety limits, and the observed behavior does not indicate any anomaly or concern.

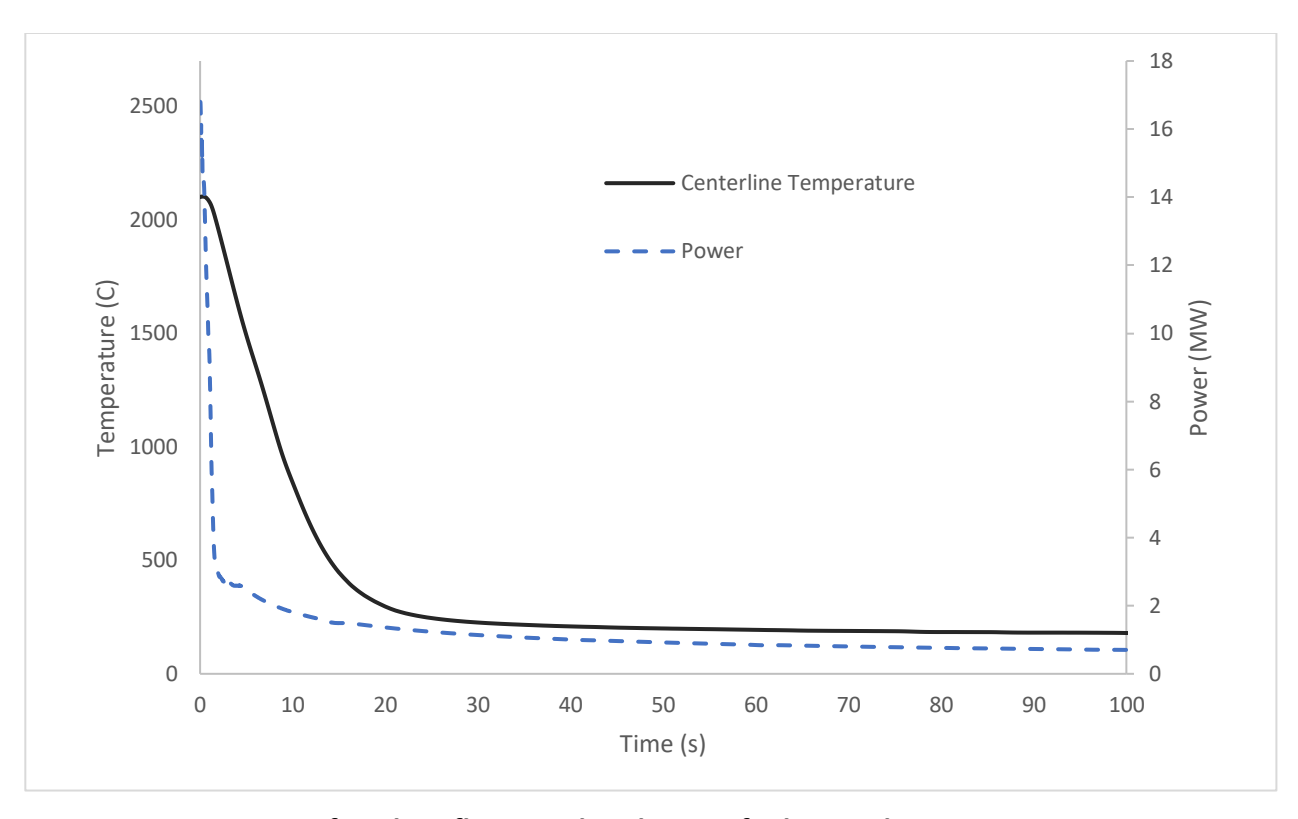


Figure 13-13: Loss of coolant flow accident hot pin fuel centerline temperature response



CHAPTER 13 ACCIDENT ANALYSES

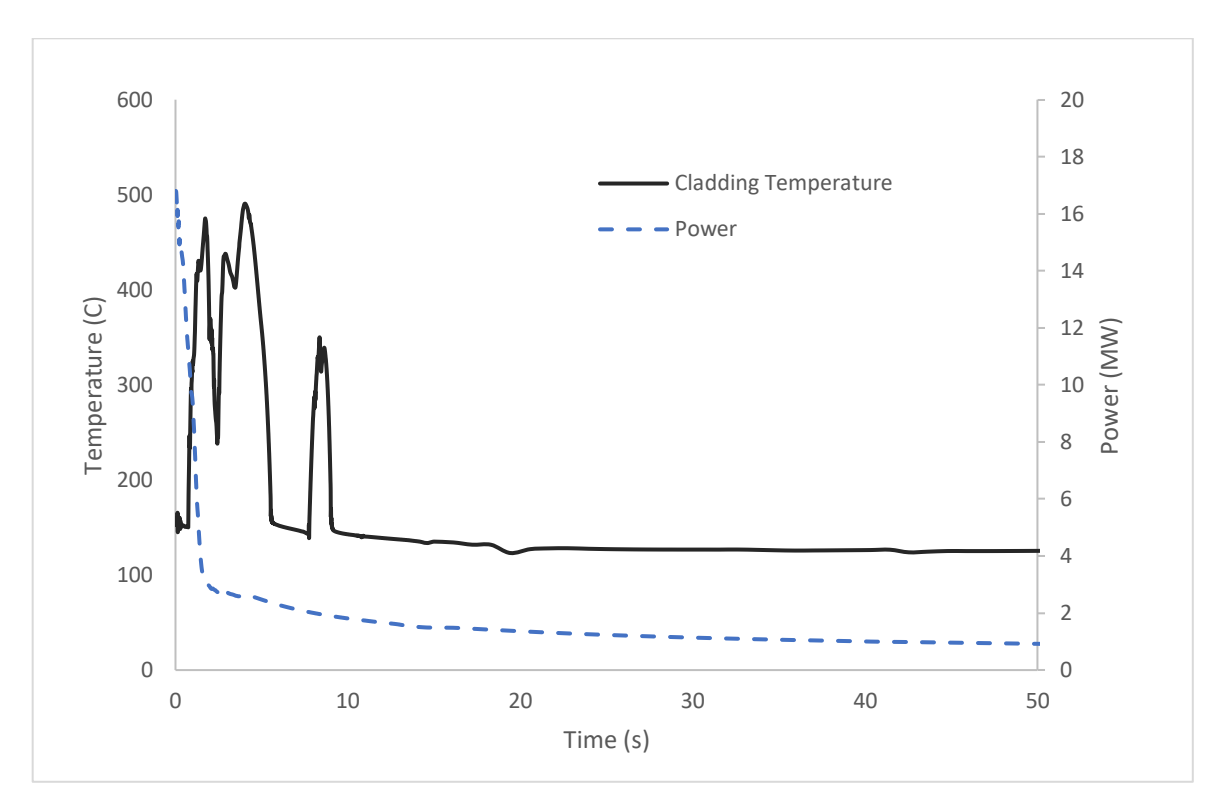


Figure 13-14: Loss of coolant flow accident hot pin cladding temperature response

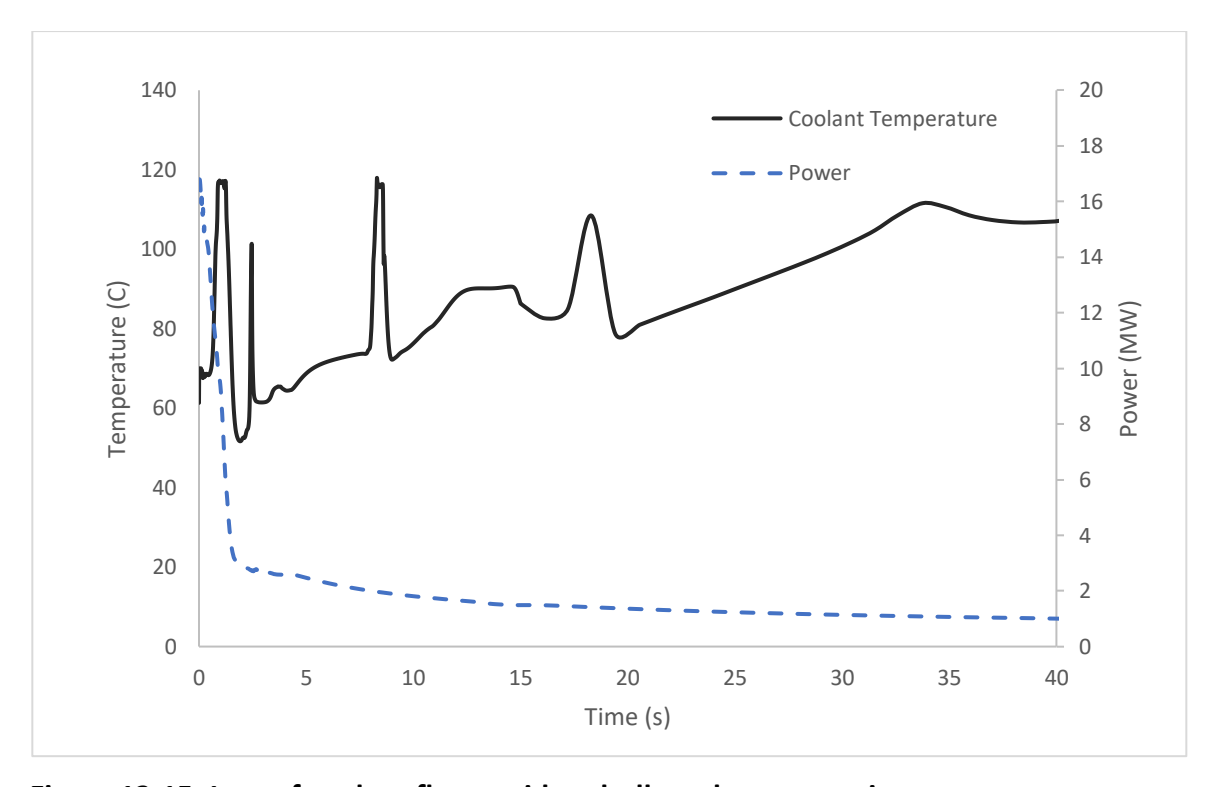


Figure 13-15: Loss of coolant flow accident bulk coolant core exit temperature response



The velocity of the coolant entering the VIPR core is shown in **Figure** 13-16. The void fraction of the coolant in the core reaches a maximum when the coolant velocity is at its minimum, as shown in **Figure** 13-16. This increased void fraction is a result of additional nucleate boiling caused by the combination of increased temperatures and decreased coolant mass flow rate and primarily occurs around the axial power peak of the hottest pins in the core. Due to the temperature-dependent reactivity feedback effects in the fuel and coolant, the falling temperatures add reactivity to the system as the power defect is removed. The control rods provide sufficient shutdown margin to ensure that the VIPR remains shut down in all conditions.

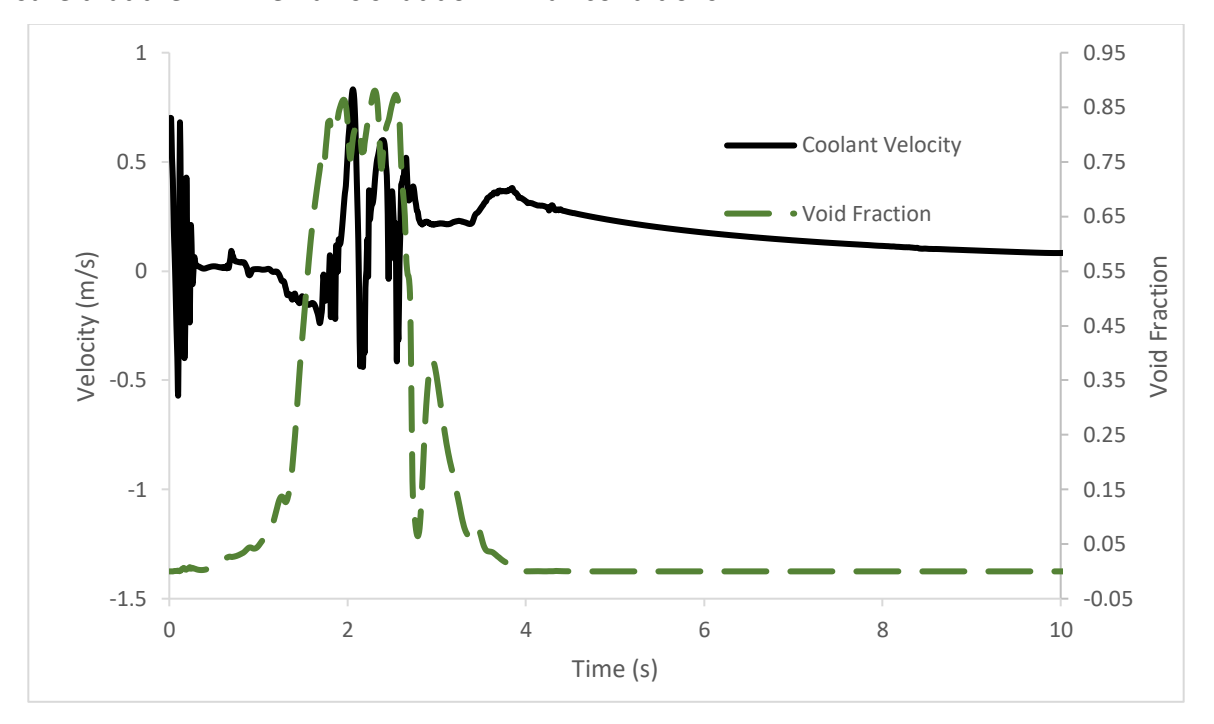


Figure 13-16: Loss of coolant flow accident bulk coolant velocity and void fraction response in the VIPR core

The fuel, cladding, and coolant all reach approximately the same temperature following the accident and reactor shutdown. With the cessation of heat removal from the secondary coolant system, all temperatures within the reactor module slowly increase without bound following the accident due to the decay heat. The predicted temperatures of the hot pin fuel centerline, hot pin cladding, and coolant over 72 hours following the accident are shown in **Figure 13-17**. The majority of the energy released over the course of the accident occurs before the reactor is shut down; because of the decay heat produced in the fuel, however, the amount of energy deposited in the system steadily increases throughout the accident.



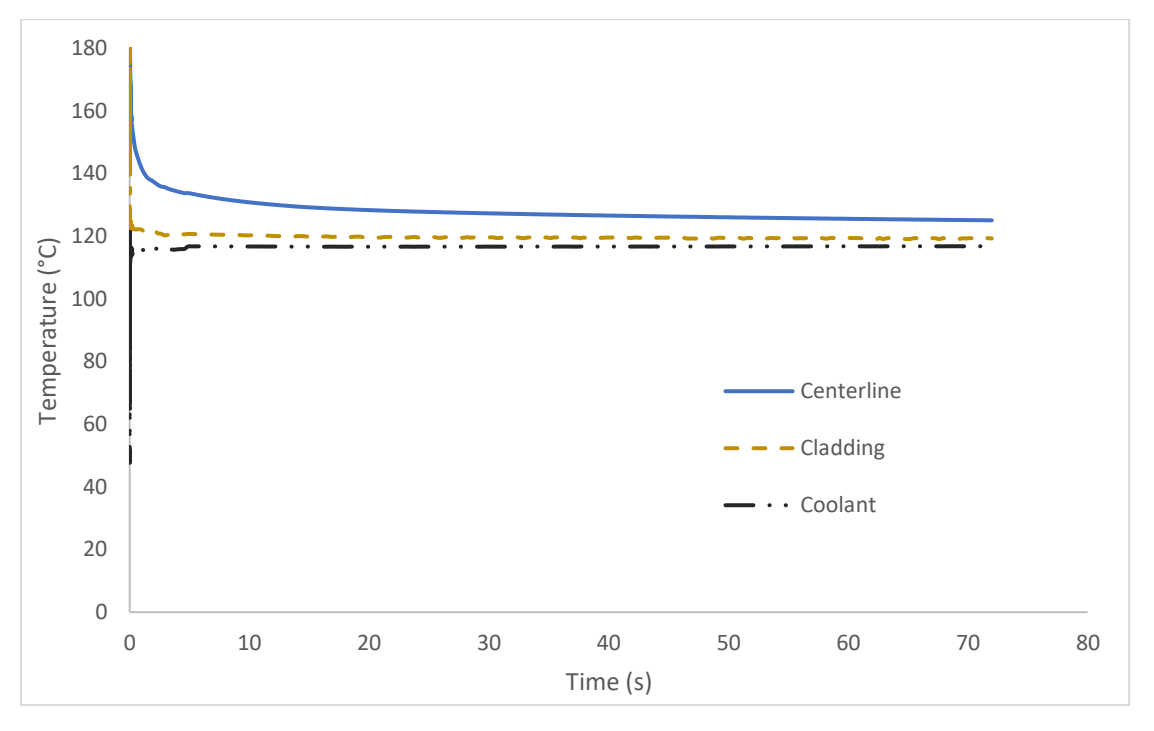


Figure 13-17: Hot pin bulk coolant temperatures following a loss of coolant flow accident

Table 13-13: Loss of coolant flow accident output parameters

Parameter	Value	Unit
Power (Maximum)	16.80	MW
Hot Pin Fuel Centerline (Maximum)	2375	°C
Hot Pin Cladding (Maximum)	475	°C
Coolant Outlet Temperature (Maximum)	118	°C

13.3.4.2.6 Barrier Performance

Because the maximum temperatures reached in the hot pin fuel centerline and cladding each remain below their respective safety limits throughout the accident, it is assumed that no fuel pin will violate either limit during the accident, and the integrity of all cladding is assured. Furthermore, as the maximum expected heat flux is less than the minimum critical heat flux no departure from nucleate boiling is anticipated, and no cladding degradation from oxidation is anticipated.

13.3.4.2.7 Radiological Consequences

As all radiological barriers are anticipated to remain intact, and all biological shielding will remain intact and undamaged, there is no radiological release anticipated from this accident.



AAI-PSAR-13 (NP) Rev 0

Page 13-47

13.3.4.3 Blocking of One or More Fuel Coolant Channels

This accident is bounded by the analysis discussed in Section 13.3.4.2, the failure of a component of the PCS. This section will be further developed in the FSAR submittal to include a topical treatment of potential initiating events.

13.3.5 Mishandling or Malfunction of Fuel

13.3.5.1 Overheating of Fuel During Steady-Power Operation

This accident is bounded by the analysis discussed by the MHA in Section 13.3.1. This section will be further developed in the FSAR submittal to include a topical treatment of potential initiating events.

13.3.5.2 Dropping or Damaging Fuel

This accident is bounded by the analysis discussed by the MHA in Section 13.3.1. This section will be further developed in the FSAR submittal to include a topical treatment of potential initiating events.

13.3.5.3 Dropping of or Impacting with a Non-Fueled Component

This accident is bounded by the analysis discussed by the MHA in Section 13.3.1. This section will be further developed in the FSAR submittal to include a topical treatment of potential initiating events.

13.3.5.4 Operation with Damaged Fuel

This accident is bounded by the analysis discussed by the MHA in Section 13.3.1. This section will be further developed in the FSAR submittal to include a topical treatment of potential initiating events.

13.3.6 <u>Experiment Malfunction</u>

13.3.6.1 Loss of Cooling Capability in a Fueled Experiment

This accident is bounded by the MHA analysis discussed in Section 13.3.1. This section will be further developed in the FSAR submittal to include a topical treatment of potential initiating events.

13.3.6.2 Mechanical Failure of a Fueled Experiment – Maximum Credible Accident

The rupture of an irradiated experiment capsule is the basis for the Maximum Credible Accident (MCA) scenario at the VIPR facility. The mechanical irradiation target failure is very similar to the fuel handling accident in that it involves special nuclear material, fission products, and release into the primary coolant. However, whereas the fuel handling accident involves a large amount of fuel, any experiment or irradiation target containing fissionable material is limited, in general, so that production of gaseous and volatile fission products results in releases lower than that considered in Section 13.3.1. Therefore, experiment malfunction will not result in consequences more severe than those listed in the MHA.

13.3.6.2.1 Initial Conditions and Methodology

This MCA postulates a mechanical failure of a fully irradiated capsule during post-irradiation handling or transport within the reactor confinement. The postulated capsule contains a conservatively bounding amount of HALEU, [] PROP,ECI of 19.75% enriched uranium metal (irradiation targets specifically for the production of Mo-99 normally involve less than [] PROP,SEC,ECI grams of uranium; the majority of targets contain no uranium), plated on a structural substrate and has undergone a representative 14-day irradiation cycle at full power (15 MWth) with no cooldown



AAI-PSAR-13 (NP) Rev 0

Page 13-48

or decay. This scenario is representative of routine medical isotope production operations and is analyzed as the MCA due to the potential for localized airborne contamination and radiological worker exposure. The reactor is shut down and decay heat is negligible. The capsule is assumed to fail while submerged in the reactor pool or a water-filled transfer facility. A complete rupture is postulated, resulting in release of fission products into the water, followed by prompt volatilization and entrainment into the confinement airspace via bubbling or aerosol transport. The confinement HVAC system is assumed to be in an inactive, passively sealed state (as building leakage is more a conservative assumption than the HVAC operating nominally with included HEPA and charcoal filtration). This event follows the methodology from the MHA (in RG 1.183 Rev. 0) but it is distinct from it as the MHA considers a full fuel assembly's failure.

13.3.6.2.2 Accident Initiator and Scenario Evolution

The initiating event is mechanical or thermal stress-induced rupture of the target capsule, possibly due to handling error, thermal shock, or embrittlement. It is assumed that 100% of the target's fission product inventory is instantaneously available for release, with isotopic masses based on bounding depletion modeling of the most highly irradiated target. Volatile radionuclides are transported from the pool to the airspace by boiling, splashing, or gas evolution. No credit is taken for decay, aerosol deposition, or water retention beyond conservative decontamination factors.

Conservatively, at the instant the capsule ruptures, fission products such as iodine and xenon, travel up through the pool water and are dispersed into the confinement air. The activity instantly dilutes to the confinement structure volume and leaks out at a volumetric leak rate. Dose consequences are calculated both to occupational staff within the confinement and to receptors at the site boundary (150 m) under conservative meteorological assumptions.

13.3.6.2.3 Sequence of Events and Timing

- 00:00:00.00: Capsule ruptures during handling
- 00:00:00.00: Gasses and volatile fission products instantly escape to pool water
- 00:00:00.00: Activity instantly transported to air volume above pool
- 30:00:00.00: Airborne radionuclides circulate in confinement volume
- 30:00:00.00: Confinement leakage to ground-level

No active mitigation is credited. Dose assessment assumes continuous worker occupancy for 2 hours post-event and passively inactive ventilation operation.

13.3.6.2.4 Barrier Failures and Releases

The breached capsule constitutes the sole failed physical barrier. The confinement structure remains intact. Conservative release fractions are applied based on Regulatory Guide 1.183 and supporting technical bases. These include:



Table 13-14: Factors from RG 1.183 Rev. 1 (2023) Table 4 and actinides

Group	Element	Gap Fraction	Pool Decontamination Factor
Noble Gases	Xe	0.06	1
	Kr-85	0.4	1
	Kr	0.06	1
Halogens	I-131	0.07	0.005
	I-132	0.07	0.005
	I	0.04	0.005
	Br	0.04	0.005
Alkali Metals	Cs	0.2	0
	Rb	0.2	0
Noble Metals	Мо	0	0
Actinides	Pu	0	0
	U	0	0

All airborne activity is assumed to mix uniformly in the confinement airspace and leak to the environment from the passively sealed, inactive building. Filter efficiency is conservatively not credited.

13.3.6.2.5 Source Term Derivation

Isotope inventories were calculated using a bounding depletion model assuming 14 days of irradiation at nominal flux conditions with no decay or cooldown prior to capsule failure. The resulting source term includes over 20 radionuclides, primarily fission products with short-to-intermediate half-lives. Airborne source terms are calculated by multiplying isotopic inventories by group-specific gap fractions and pool decontamination factors.

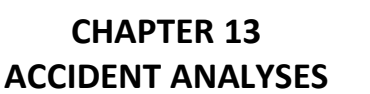
13.3.6.2.6 Occupational Dose Calculation

Inhalation and immersion doses to workers are evaluated using Bq/m³ airborne concentrations, inhalation DCFs from Federal Guidance Report (FGR) 11, "Limiting Values of Radionuclide Intake and Air Concentration and Dose Conversion Factors for Inhalation, Submersion, and Ingestion," Rev 0, September 1988, Table 2.1, and immersion DCFs from FGR 12, "External Exposure to Radionuclides in Air, Water, and Soil," Rev 0, September 1993, Table III.1. A breathing rate of 3.5E-4 m³/s and an exposure duration of 2 hours are assumed. The isotopes decay and leak from confinement over time, but no deposition to the walls or ground is credited.

13.3.6.2.7 Offsite Dose Calculation

Unfiltered, decaying airborne activity leaks from the confinement and delivers doss to the nearest site boundary receptor at 150 m. The Total Effective Dose Equivalent is the sum of immersion and inhalation doses – Effective Dose Equivalent and Committed Effective Dose Equivalent – and is







evaluated using 0.5% exceedance χ/Q . The χ/Q for the highest 24-, and 96-hour maximum dose periods are determined, as consistent with RG 1.183 Appendix B. The total dose committed to the thyroid and the total effective dose at each timestep were calculated by summing the individual contributions of all radionuclides. The total dose over the accident was obtained by summing the dose uptake at all timesteps. TEDE is calculated as:

$$TEDE = A_{released} \times \frac{X}{Q} \times (EDE_{FGR12} + CEDE_{FGR11} \times BR(t))$$

13.3.6.2.8 Occupational and Offsite Dose Results

Table 13-15: Occupational and offsite TEDE and thyroid dose results from the MCA

Receptor	Dose (rem)	Assumptions
TEDE for a Worker (confinement, 2 hr)	2.44E+00	Full inhalation, no personal protective equipment, conservative breathing rate
TEDE for Site Boundary (24 hr, 150 m)	1.16E-03	0.5% χ/Q, pool decontamination except noble gases
TEDE for Site Boundary (96 hr, 150 m)	2.08E-03	0.5% χ/Q, pool decontamination except noble gases
Thyroid Dose at Site Boundary (96, 150 m)	4.33E-02	0.5% χ/Q, pool decontamination except noble gases

Doses are well below regulatory thresholds for licensing and emergency planning.

13.3.6.2.9 Comparison to Dose Acceptance Criteria

The analysis results are compared to values given in ANSI/ANS-15.16-2015 which prescribes the size of an emergency planning zone (EPZ) around the facility, when appropriate.

Table 13-16: Comparison of dose results to acceptance criteria and outcomes

Criterion	Limit (rem)	Result (rem)	Outcome	Basis
Worker annual TEDE (2 hr)	5.0	2.44E+00	Design basis safe and within regulatory limits	10 CFR 20.1201
Public TEDE at site boundary (24 hr)	1.0	1.16E-03	Design basis safe and within regulatory limits	NUREG-0396, RG 1.183
Early-phase TEDE EPA PAG (96 hr)	1.0	2.08E-03	No need for an EPZ per EPA PAG	ANSI/ANS-15.16-2015, EPA-400-R-17-001
Early-phase Thyroid Dose EPA PAG (96 hr)	5.0	4.33E-02	No need for an EPZ per EPA PAG	ANSI/ANS-15.16-2015, EPA-400-R-17-001



AAI-PSAR-13 (NP) Rev 0

Page 13-51

ANSI/ANS-15.16-2015 states that, "As part of emergency planning, the reactor licensee or owner/operator of a facility that identifies radiological emergencies that result in off-site plume exposures exceeding 10 mSv deep dose (1 rem whole body) or 50 mSv (5 rem) thyroid shall identify an EPZ." As the MCA doses are well below the EPZ thresholds no plume exposure pathway EPZ is required.

While emergency planning is provided for the Meitner-1 facility, this accident analysis supports the conclusion that the MCA does not warrant a formal EPZ. All calculated doses remain within acceptable limits defined in 10 CFR Part 20, "Standards for Protections Against Radiation," 10 CFR Part 100, "Reactor Site Criteria," and applicable guidance documents.

13.3.6.3 Loss of Cooling Capability in a Strongly Absorbing Non-Fueled Experiment

This accident is bounded by the MHA analysis discussed in Section 13.3.1. This section will be further developed in the FSAR submittal to include a topical treatment of potential initiating events.

13.3.6.4 Placement of an Experiment Component in an Unplanned Location

This accident is bounded by the MHA analysis discussed in Section 13.3.1. This section will be further developed in the FSAR submittal to include a topical treatment of potential initiating events.

13.3.6.5 Failure of an Experiment Containing Highly Reactive Contents

This accident is bounded by the MHA analysis discussed in Section 13.3.1. This section will be further developed in the FSAR submittal to include a topical treatment of potential initiating events.

13.3.6.6 Failure of an Experiment and Release of Corrosive Materials into the Reactor Coolant

This accident is bounded by the MHA analysis discussed in Section 13.3.1. This section will be further developed in the FSAR submittal to include a topical treatment of potential initiating events.

13.3.6.7 Detonation of an Explosive Experiment

This accident is bounded by the MHA analysis discussed in Section 13.3.1. This section will be further developed in the FSAR submittal to include a topical treatment of potential initiating events.

13.3.7 Loss of Normal Electrical Power

This accident is bounded by the analysis discussed in Section 13.3.4.2, the failure of a component of the PCS. This section will be further developed in the FSAR submittal to include a topical treatment of potential initiating events.

13.3.8 External Events

13.3.8.1 Meteorological Disturbance

The AAI Non-Power Production or Utilization Facility (NPUF) is designed to withstand extreme meteorological events. In the event that the building structure is damaged, it is unlikely that equipment which performs a safety function inside the facility would be damaged as well. The biological shield is not susceptible to meteorological damage. Any safety instrumentation will be in the reactor pool, and the control rods fail-safe into the core if building damage were to affect the control rod drive mechanism and associated subsystems.



AAI-PSAR-13 (NP) Rev 0

Page 13-52

13.3.8.2 Seismic Event

Structures, systems, and components (SSCs) which perform a safety function are designed to withstand seismic events with heightened requirements; see Chapter 3, Section 3.4 for AAI's seismic damage SSC classifications. Seismic monitors, which are not credited with a safety function, will initiate safe shutdown of the reactor on the primary wave, well before the destructive secondary wave would reach the facility. Seismic monitors are discussed further in Chapter 3, Section 3.4.

13.3.8.3 Mechanical Impact or Collision with Building

The AAI NPUF has a fenced boundary and a security checkpoint which only allows specific vehicle traffic near the facility. All external bay doors for inserting or removing equipment are located at the shipping and receiving area or the reactor auxiliary area, mitigating potential collisions with the confinement structure or the production facility walls. A fire lane follows the perimeter of the facility, but is offset from the building, mitigating the likelihood of an emergency vehicle impacting the building (see Chapter 1, Figure 1-3). Generally, slow speed limits within the site fence line preclude damaging the facility structure in the unlikely event of an impact.

There are no SSCs which perform a safety function on the immediate opposite side of any outer facility walls which are accessible via road/lot.

13.3.9 Mishandling or Malfunction of Equipment

13.3.9.1 Operator Error at the Controls

Errors made by an operator at the controls could conceivably result in the continuous removal of a control rod assembly up to the maximum rate, a change in the operating parameters of the reactor coolant system, or the cessation of forced convective flow of the reactor coolant. These accidents' respective initiating events are bounded by the accident analyses discussed in Section 13.3.2.4, Section 13.3.2.6, and Section 13.3.4.2.

13.3.9.2 Other Operator Errors

In addition to the initiating events discussed in Section 13.3.9.1, an operator could conceivably be responsible for the following:

- Rapid insertion of a fuel assembly into a core vacancy
- Damage to or failure of the reactor coolant boundary
- Blocking of one or more fuel coolant channels
- Dropping or damaging fuel, dropping non-fueled components, or operating with damaged fuel
- Any experiment malfunction

These accidents are bounded by the accident analyses discussed in Section 13.3.2.3, Section 13.3.3.4, Section 13.3.4.3, and Section 13.3.5, and by the experiment accident analyses discussed in Section 13.3.6.

13.3.9.3 Malfunction or Loss of Safety-Related Instruments or Controls

Malfunction of instruments or controls which perform a safety function could conceivably result in consequences identical to those presented in Section 13.3.9.1. Loss of these instruments or controls



AAI-PSAR-13 (NP) Rev 0

Page 13-53

would result in an immediate reactor scram through independent, isolated systems, the consequences of which are bounded by the accident analyses discussed in Section 13.3.2.4, Section 13.3.2.6, and Section 13.3.4.2.

13.3.9.4 Electrical Fault in Control Rod Systems

An electrical fault in the control rod systems could result in consequences ranging from a loss of electrical power to one or more control rod systems, resulting in an immediate reactor scram, up to the continuous removal of a control rod assembly at the maximum rate, bounded by the accident analysis discussed in Section 13.3.2.4.

13.3.9.5 Malfunction of Confinement or Containment System

Malfunction of or damage to the confinement constitutes a reduction in defense-in-depth and does not inherently imply a radiological release.

13.3.9.6 Rapid Leak of Contaminated Liquid

This accident is bounded by the MHA analysis discussed in Section 13.3.1.

13.4 SUMMARY AND CONCLUSIONS

The analyses and results presented in this chapter show the robust nature of the VIPR, and how the passive design elements ensure that fuel cladding integrity is maintained in a spectrum of challenging scenarios. The incredible event of stripping cladding from every fuel rod in an AAI [

]PROP,ECI fuel assembly was employed as a bounding maximum hypothetical accident for radiological release. With an unmitigated consequence of a TEDE at 150 m of just 34% of the 1 rem criteria set forth in 10 CFR 50.34(a)(1)(i), AAI shows that even with highly conservative and hypothetical accident assumptions, the AAI NPUF can be safely operated. Using the same methodology as the MHA in a maximum credible accident scenario of a fueled target failure, the design bases are proven to provide safety up to and including for the worst accidents that could credibly happen. With a conservatively-derived dose to offsite receptors at the 150 m site boundary of 0.15% of the regulatory set point of 1 rem the MCA analysis shows the efficacy of the engineered safety features and inherent safety of the VIPR facility design.

13.5 REFERENCES

- American Nuclear Society. 2020. ANSI/ANS-6.1.1-2020, "Photon and Neutron Fluence-To-Dose Conversion Coefficients." American National Standards Institute.
- ——— ANSI/ANS-15.16-2015, "Emergency Planning for Research Reactors." American National Standards Institute.

Idaho National Laboratory. 2018. RELAP5-3D. V. 4.4.2. Idaho National Laboratory. Linux.

International Atomic Energy Agency (IAEA). 2008. Safety Report Series No.53, "Derivation of the Source Term and Analysis of the Radiological Consequences of Research Reactor Accidents." http://www-pub.iaea.org/MTCD/publications/PDF/Pub1308_web.pdf.



AAI-PSAR-13 (NP) Rev 0

Page 13-54

- International Atomic Energy Agency (IAEA). 1999-2005. Final Report of a Coordinated Research Project, "Thermophysical properties database of materials for light water reactors and heavy water reactors." IAEA-TECDOC-1496.

 https://www-pub.iaea.org/MTCD/Publications/PDF/te 1496 web.pdf.
- Leppänen, J., M. Pusa, T. Viitanen, V. Valtavirta, and T. Kaltiaisenaho. 2015. "The Serpent Monte Carlo code: Status, development and applications in 2013." Ann. Nucl. Energy, 82: 142-150.
- National Oceanic and Atmospheric Administration. 1974. Technical Memorandum ERL ARL-42, "A Program for Evaluation Atmospheric Dispersion From a Nuclear Power Station." (June)
- Nuclear Regulatory Commission. 1996. NUREG-1537, Part 1, "Guidelines for Preparing and Reviewing Applications for the Licensing of Non-Power Reactors, Format and Content."
- Nuclear Regulatory Commission. 2014. NUREG/CR-7024, Rev. 1, "Fuel Fragmentation, Relocation, and Dispersal during the Loss-of-Coolant Accident." https://www.nrc.gov/reading-rm/doccollections/nuregs/contract/cr7024
- Todreas, Neil E., and Mujid S. Kazimi. 2021. *Nuclear systems volume I: Thermal hydraulic fundamentals.* CRC press, 2021.
- Werner, C. J. (editor). 2017. "MCNP Users Manual Code Version 6.2", Los Alamos National Laboratory, Report LA-UR-17-29981.
- Westinghouse Electric Co. 2011. "Accident Analysis." *AP1000 Design Control Document*, Chapter 15, Rev. 19. (June) https://www.nrc.gov/docs/ML1117/ML11171A374.pdf